



**Calhoun: The NPS Institutional Archive**  
**DSpace Repository**

---

Theses and Dissertations

1. Thesis and Dissertation Collection, all items

---

1986

# The effect of thermomechanical processing variables on ductility of a high-Mg, Al-Mg-Zr alloy.

Grider, William H., Jr.

---

<http://hdl.handle.net/10945/21809>

---

This publication is a work of the U.S. Government as defined in Title 17, United States Code, Section 101. Copyright protection is not available for this work in the United States.

*Downloaded from NPS Archive: Calhoun*



Calhoun is the Naval Postgraduate School's public access digital repository for research materials and institutional publications created by the NPS community. Calhoun is named for Professor of Mathematics Guy K. Calhoun, NPS's first appointed -- and published -- scholarly author.

**Dudley Knox Library / Naval Postgraduate School**  
**411 Dyer Road / 1 University Circle**  
**Monterey, California USA 93943**

<http://www.nps.edu/library>







DUDLEY KNOX LIBRARY  
NAVAL POSTGRADUATE SCHOOL  
MONTEREY, CALIFORNIA 93943-5002















# NAVAL POSTGRADUATE SCHOOL

Monterey, California



## THESIS

THE EFFECT OF  
THERMOMECHANICAL PROCESSING VARIABLES  
ON DUCTILITY OF A HIGH-Mg, Al-Mg-Zr ALLOY

by

William H. Grider, Jr.  
June 1986

Thesis Advisor:

T.R. McNelley

Approved for public release; distribution is unlimited.

T230601



# REPORT DOCUMENTATION PAGE

REPORT SECURITY CLASSIFICATION UNCLASSIFIED		1b. RESTRICTIVE MARKINGS	
SECURITY CLASSIFICATION AUTHORITY		3 DISTRIBUTION / AVAILABILITY OF REPORT Approved for public release; distribution is unlimited.	
DECLASSIFICATION / DOWNGRADING SCHEDULE		5 MONITORING ORGANIZATION REPORT NUMBER(S)	
PERFORMING ORGANIZATION REPORT NUMBER(S)		7a. NAME OF MONITORING ORGANIZATION Naval Postgraduate School	
NAME OF PERFORMING ORGANIZATION Naval Postgraduate School	6b OFFICE SYMBOL (If applicable) 69	7b. ADDRESS (City, State, and ZIP Code) Monterey, California 93943-5000	
ADDRESS (City, State, and ZIP Code) Monterey, California 93943-5000		9. PROCUREMENT INSTRUMENT IDENTIFICATION NUMBER	
NAME OF FUNDING / SPONSORING ORGANIZATION	8b. OFFICE SYMBOL (If applicable)	10 SOURCE OF FUNDING NUMBERS	
ADDRESS (City, State, and ZIP Code)		PROGRAM ELEMENT NO	PROJECT NO
		TASK NO	WORK UNIT ACCESSION NO

TITLE (Include Security Classification) THE EFFECT OF THERMOMECHANICAL PROCESSING VARIABLES ON DUCTILITY OF A HIGH-Mg, Al-Mg-Zr ALLOY

PERSONAL AUTHOR(S)  
William H. Grider, Jr.

1 TYPE OF REPORT Master's Thesis	13b TIME COVERED FROM TO	14 DATE OF REPORT (Year, Month, Day) 1986 June	15 PAGE COUNT 78
-------------------------------------	-----------------------------	---	---------------------

SUPPLEMENTARY NOTATION

COSATI CODES			18 SUBJECT TERMS (Continue on reverse if necessary and identify by block number)  Superplasticity, Ductility, Aluminum-Magnesium Alloys, Thermomechanical Processing
FIELD	GROUP	SUB-GROUP	

ABSTRACT (Continue on reverse if necessary and identify by block number)

In previous research on thermomechanically processed high - Mg, Al - Mg alloys, yield strengths of 276 MPa (40 ksi) were retained after simulated superplastic forming, but ductility at ambient temperature varied from one to fourteen percent elongation in tension testing. This variability in ductility was studied in a series of experiments conducted on an Al-10%Mg-0.1%Zr alloy. Study by light microscopy and scanning electron microscopy revealed defects resulting from inverse segregation in the original casting and also defects resulting from the relatively light reductions utilized in the warm rolling of the material. The use of heavier reductions in rolling was shown to improve tensile ductility at ambient temperature both in the as-rolled and annealed conditions. Superplasticity in material processed using such heavier reductions in rolling was then studied by tension testing at 300°C.

DISTRIBUTION / AVAILABILITY OF ABSTRACT <input type="checkbox"/> UNCLASSIFIED/UNLIMITED <input type="checkbox"/> SAME AS RPT <input type="checkbox"/> DTIC USERS		21 ABSTRACT SECURITY CLASSIFICATION Unclassified	
a NAME OF RESPONSIBLE INDIVIDUAL T.R. McNelley		22b TELEPHONE (Include Area Code) (408) 646-2589	22c OFFICE SYMBOL 69MC

Approved for public release; distribution is unlimited.

The Effect of Thermomechanical Processing Variables on Ductility  
of a High-Mg, Al-Mg-Zr Alloy

by

William H. Grider, Jr.  
Lieutenant, United States Navy  
B.S., U.S. Naval Academy, 1979

Submitted in partial fulfillment of the  
requirements for the degree of

MASTER OF SCIENCE IN MECHANICAL ENGINEERING

from the

NAVAL POSTGRADUATE SCHOOL  
June 1986



## ABSTRACT

In previous research on thermomechanically processed high - Mg, Al- Mg alloys, yield strengths of 276 MPa (40ksi) were retained after simulated superplastic forming, but ductility at ambient temperature varied from one to fourteen percent elongation in tension testing. This variability in ductility was studied in a series of experiments conducted on an Al-10%Mg-0.1%Zr alloy. Study by light microscopy and scanning electron microscopy revealed defects resulting from inverse segregation in the original casting and also defects resulting from the relatively light reductions utilized in the warm rolling of the material. The use of heavier reductions in rolling was shown to improve tensile ductility at ambient temperature both in the as-rolled and annealed conditions. Superplasticity in material processed using such heavier reductions in rolling was then studied by tension testing at 300°C.

## TABLE OF CONTENTS

I.	INTRODUCTION -----	12
	A. ALUMINUM-MAGNESIUM ALLOYS -----	12
	B. HIGH-MAGNESIUM ALLOYS -----	12
	C. SUPERPLASTICITY -----	13
	D. DUCTILITY PROBLEMS -----	14
II.	BACKGROUND -----	16
	A. METALLURGY OF ALUMINUM-MAGNESIUM ALLOYS ----	16
	1. Phases and Solubility -----	16
	2. Ternary Additions -----	16
	3. Solidification Defects -----	18
	B. ROLLING -----	18
	C. MICROSTRUCTURAL CHARACTERISTICS -----	19
	1. Microstructure at Ambient Temperature---	19
	2. Strengthening Mechanisms -----	20
	D. SUPERPLASTIC BEHAVIOR -----	20
	E. WHY THE PRESENT WORK -----	22
	1. Purpose -----	22
	2. Approach-----	23
III.	EXPERIMENTAL PROCEDURE -----	24
	A. MATERIAL -----	24
	B. PROCESSING -----	24
	C. WARM ROLLING -----	26
	D. AMBIENT AND ELEVATED TEMPERATURE TESTING----	27
	E. DATA REDUCTION -----	29
	F. METALLOGRAPHY -----	29

IV.	RESULTS -----	32
A.	METALLOGRAPHIC CHARACTERIZATION -----	32
1.	As-Cast Microstructure -----	32
2.	Solution Treated Microstructure -----	33
3.	Upset Forged Condition -----	33
4.	Warm Rolled Condition -----	37
B.	MECHANICAL TESTING -----	45
1.	Ambient Temperature Testing -----	45
2.	Elevated Temperature Testing -----	56
a.	Stress-Strain Response -----	56
b.	Stress-Strain Rate Data -----	59
c.	Ductility-Strain Rate Data -----	63
V.	DISCUSSION -----	65
A.	EFFECT OF ROLLING REDUCTION ON MICROSTRUCTURE -----	65
B.	EFFECT OF ROLLING REDUCTION ON AMBIENT TEMPERATURE DUCTILITY -----	66
C.	EFFECT OF ROLLING REDUCTION ON ELEVATED TEMPERATURE DUCTILITY -----	67
VI.	CONCLUSIONS AND RECOMMENDATIONS -----	68
APPENDIX A.	MECHANICAL TEST DATA ON Al-10%Mg-0.1%Zr ALLOY -----	70
APPENDIX B.	COMPUTER PROGRAM -----	73
	LIST OF REFERENCES -----	74
	INITIAL DISTRIBUTION LIST -----	77

## LIST OF TABLES

I.	ALLOY COMPOSITION (WEIGHT PERCENT) -----	24
II.	AMBIENT TEMPERATURE MECHANICAL TEST DATA OF Al-10%Mg-0.1%Zr ALLOY IN THE AS-ROLLED CONDITION (LIGHT REDUCTION PROCESSING) AND FOR ANNEALING TIMES AT 300°C -----	46
III.	AMBIENT TEMPERATURE MECHANICAL TEST DATA FOR THE Al-10%Mg-0.1%Zr ALLOY IN THE AS-ROLLED CONDITION (HEAVY REDUCTION PROCESSING) AND FOR VARIOUS ANNEALING TIMES AT 300°C -----	50
IV.	MECHANICAL TEST DATA FOR THE Al-10%Mg-0.1%Zr ALLOY, TESTED AT 300°C IN THE AS-ROLLED CONDITION, AND FOLLOWING VARIOUS ANNEALING TREATMENTS PRIOR TO ELEVATED TEMPERATURE TESTING -----	60

## LIST OF FIGURES

2.1	Aluminum-Magnesium phase diagram. The arrow indicates processing temperature for the 10 pct. Mg alloys -----	17
3.1	Schematic of the thermomechanical processing technique -----	25
4.1	SEM micrographs of an Al-10%Mg-0.1%Zr alloy, solution treated for 5 hrs. at 440°C and then 19 hrs. at 480°C. Specimen is located 1.0 cm. from ingot's outer surface; (a) dendritic solidification in secondary electron imaging mode; (b) back scattering mode reveals many Mg <sub>5</sub> Al <sub>8</sub> (white particles) and a few ZrAl <sub>3</sub> , (black particles) -----	34
4.2	Schematic illustrating sectioning for metallographic examination -----	35
4.3	Optical micrographs of an Al-10%Mg-0.1%Zr alloy solution treated, upset forged and oil quenched: (a) under cross polarized light showing equiaxed grain structure and homogeneous dispersion of second phase; (b) bright field micrograph outer edge of upset forged; the specimen showing intergranular cracking caused by inverse segregation -----	36
4.4	Optical micrograph of an Al-10%Mg-0.1%Zr alloy solution treated, upset forged and oil quenched. An intergranular crack initiated on outer edge of the specimen is shown. Also seen is a region of finer grain structure, likely a result of inverse segregation of Zr -----	38
4.5	Tri-planar micrographs of an Al-10%Mg-0.1%Zr alloy warm rolled at 300°C to a true strain of 2.2 (89 percent reduction); (a) center of rolled specimen, (b) outer edge of rolled specimen -----	39



4.6	Optical micrograph of an Al-10%Mg-0.1%Zr alloy warm rolled at 300°C to 89 percent reduction utilizing light reduction in rolling. Inverse segregation coupled with low rolling reduction facilitated edge cracking, resulting in transgranular cracking, especially in regions near the original cast surface -----	40
4.7	Optical micrographs of warm rolled Al-10%Mg-0.1%Zr alloy, tensile tested at ambient temperature; (a) light reduction showing fine, uniform distribution of second phase, (b) heavy reduction specimen, finer second phase, but less uniform distribution of beta phase -----	42
4.8	Photographs of 300°C warm rolled specimens showing (a) alligatoring due to light reduction during processing and (b) edge of same sample revealing non-uniform working of material-----	43
4.9	Photographs of 300°C warm rolled specimens showing (a) elimination of alligatoring in heavy reduction material and (b) uniform working of material typical of heavy reduction -----	44
4.10	Results of ambient temperature tension testing of material processed as in previous work; (a) and (b) are the results of the first series of tests, while (c) and (d) are the second series of tests -----	48
4.11	Results of ambient temperature tension testing of heavy reduction processed material; (a) and (b) are the results of the third series of tests -----	51
4.12	Engineering stress versus engineering strain for an ambient temperature tension test on as-rolled material showing a comparison between heavy and light reduction processing of material -----	52
4.13	SEM micrographs of a test specimen tension tested at ambient temperature following light reduction processing. Ductility was 6.0 percent elongation to fracture; fracture surface at (a) 24X, (b) 1000X, (c) 4000X. -----	54

- 4.14 SEM micrographs of a test specimen tension tested at ambient temperature following heavy reduction processing. Ductility was 19.0 percent elongation to fracture; fracture surface: (a) 26.5X, (b) 1000X, (c) 4000X ----- 55
- 4.15 SEM micrographs of test specimen tension tested at ambient temperature; (a) light reduction specimen showing a one micron beta particle in a dimple, (b) heavy reduction specimen showing no visible beta particles associated with dimples on the fracture surface ----- 57
- 4.16 Tension testing conducted at 300°C for Al-10%Mg-0.1%Zr warm rolled at 85 percent reduction using heavy reduction processing of the material; (b) engineering stress versus engineering strain; (b) true stress versus true strain ----- 58
- 4.17 True stress at 0.1 strain versus strain rate for the Al-10%Mg-0.1%Zr alloy tension tested at 300°C. Specimens were warm rolled at 300°C to 85 percent reduction using the heavy reduction processing of material. Compare with previous data, (the previous material was warm rolled at 300°C to 92 percent reduction using a light reduction scheme); the heavy reduction material was tested at various annealed temperatures and times ----- 62
- 4.18 Ductility versus strain rate for tension testing conducted at 300°C on the Al-10%Mg-0.1%Zr alloy. Comparison between previous work on as-rolled light reduction processing of material warm rolled at 300°C to 92 percent reduction to a heavy reduction processing of material warm rolled at 300°C to 85 percent reduction. The heavy reduction specimens were also tested in as-rolled and at various annealing temperatures and times ----- 64

- A.1 Engineering stress versus engineering strain data for tension testing conducted at 300°C for the heavy reduction processing material warm rolled at 300°C to 85 percent reduction: (a) annealed 1 hr. at 200°C, (b) annealed 10 hrs. at 200°C, (c) annealed 1 hr. at 300°C.---70
- A.2 True stress versus true strain data for tension testing conducted at 300°C for the heavy reduction processing material warm rolled at 300°C to 85 percent reduction: (a) annealed 1 hr. at 200°C, (b) annealed 10 hrs. at 200°C, (c) annealed 1 hr. at 300°C. -----71
- A.3 True stress at 0.1 strain versus true strain data for tension test conducted at 300°C; specimens warm rolled at 300°C to 85 percent reduction using the heavy reduction processing of material. Comparison is made with previous data, the previous material was warm rolled at 300°C to 92 percent reduction using a light reduction scheme. The heavy reduction specimens were also annealed at various temperatures and times -----72

## ACKNOWLEDGEMENT

I would like to thank my advisor, Professor T.R. McNelley and Dr. S.J. Hales for their expert assistance and guidance in conducting this research. Also T. McCord, T. Kellogg, Tamara Bloomer whose technical expertise, material support and knowledge were vital to me in the experimental portion of this thesis. Finally, I would like to express my sincere appreciation to my wife, Cheri' and our two children Christina and Stephanie for their dedicated support of my work at NPS.

## I. INTRODUCTION

### A. ALUMINUM-MAGNESIUM ALLOYS

Aluminum-Magnesium alloys generally are strengthened by Mg in solid solution, strain hardening and grain size control. At high-Mg levels, precipitation of  $Mg_5Al_8$  may occur but relative little strengthening results as it is insufficiently fine. In industry, Aluminum-Magnesium alloy typically contain less than six percent Mg. These alloys are often used when weight becomes an important factor, as in transportation applications. For example, 5XXX series alloys are low in strength as compared to age hardened Al alloys but have good fatigue, fracture, weldability and stress corrosion characteristics. A disadvantage with the Aluminum-Magnesium alloys is low melting temperature which prevents their use in elevated temperature environments.

[Ref. 1]

### B. HIGH-MAGNESIUM ALLOYS

High-Mg alloys have been extensively studied at NPS. The advantages of a high magnesium alloys include: 1) moderate to high strength; 2) lower density than other high strength Al alloys; 3) good ductility; 4) good toughness; 5) corrosion resistance when properly processed; and 6) good high cycle fatigue behavior. In contrast, the main disadvantage is a potential loss in fatigue resistance and



stress-corrosion cracking susceptibility at high Mg-levels when Mg-precipitation is inadequately controlled.

Previous research with 8-10% Mg, Al-Mg alloys by Johnson and Shirah [Ref. 2, 3] resulted in a thermomechanical process (TMP) to enhance stress-corrosion resistance, fatigue resistance and improve both ambient and elevated temperature properties. The essential features of the TMP are: 1) solution treatment above the solvus to dissolve all soluble components; 2) hot working by upset forging to further refine and homogenize the microstructure; 3) quenching from solution treatment to provide a metastable structure [Ref. 4] and 4) reheating and warm working to large strains at a temperature below the Mg-solvus. This provides for a fine dispersion of the beta phase,  $(\text{Mg}_5\text{Al}_8)$ , and increases strength through a combination of dislocation substructure, dispersion and solid solution strengthening.

### C. SUPERPLASTICITY

The phenomenon of superplasticity in metals was first demonstrated in a ternary eutectic alloys by Rosenhain [Ref. 5] in 1920. Since then, a large amount of research has been accomplished. However, much remains to be learned about the mechanisms that facilitate deforming of specimens in tension at extremely low stresses with essentially neck free elongations of several hundred or several thousand percent.

The need exists for both military and commercial metallic alloys of high ambient temperature strength and also the unique fluid-like warm temperature deformation characteristics of hot polymers and glasses. Indeed, they may be essential as alternatives to present day conventional metal deformation processing for some complex, high performance structures.

The many opportunities available for superplastic alloy application include: 1) application of thermoplastic sheet forming methods; 2) ability to produce deep and complex shapes in one single operation, which reduces the cost of tooling; 3) eliminating the need for fasteners or welding which not only increases component strength but also decreases the component's weight; 4) a high strength and good corrosion resistance, as a result of the fine microstructure acquire in superplastic processing. [Ref. 6]

#### D. DUCTILITY PROBLEMS

In previous thesis research examining simulated superplastic forming, ductilities of the Al-10%Mg-0.1%Zr alloy varied widely with no apparent correlation to prior thermo-mechanical processing. During ambient temperature tension testing of rolled or rolled and annealed material, ductilities ranged from 4.9% to 10.5%. After simulated superplastic forming, the ambient temperature ductilities ranged from 1.0% to 14.2%. Detailed optical microscopy by Klankowski [Ref. 7] did not reveal the cause of this problem. This

present work was then directed at investigating the effect of thermomechanical processing variables on ductility of an Al-10%Mg-0.1%Zr.

## II. BACKGROUND

### A. METALLURGY OF ALUMINUM-MAGNESIUM ALLOYS

#### 1. Phases and Solubility

Figure 2.1 shows the Al-Mg binary phase diagram. Under ordinary processing conditions, most Mg present may be retained in solution for alloys up to six percent Mg and hence strengthening is primarily by the solid solution mechanism. As Mg-content is increased beyond six percent, density of the alloy decreases with an attendant increase in strength to weight ratio. At the same time, the  $Mg_5Al_8$  will have an increased tendency to form, possibly resulting in age hardening but also leading to stress corrosion susceptibility if such precipitation occurs on grain boundaries. At high Mg-levels, it is suggested [Ref. 8] that dynamic recrystallization will occur during hot working; this would assist in microstructural refinement and thus in achieving more uniform distribution of the precipitate.

#### 2. Ternary Additions

A ternary addition of Zirconium was chosen to provide grain refinement via fine  $ZrAl_3$  dispersoids without adversely affecting the Mg-solubility and thus the mechanical properties of the alloy.

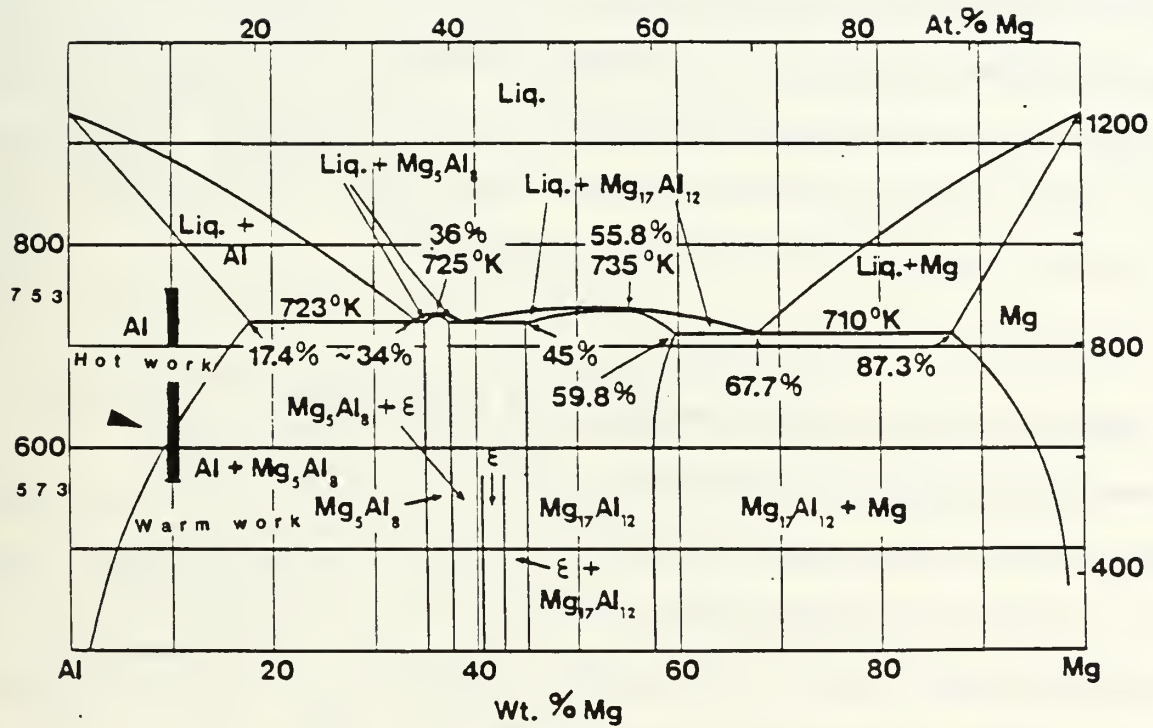


Figure 2.1. Aluminum-Magnesium phase diagram. The arrow indicates processing temperature for the 10 pct. Mag alloys.



### 3. Solidification Defects

Solidification defects of concern during TMP are hot shortness resulting from heating above the eutectic temperature but below the solidus temperature; such heating may improve homogenization but may also melt non-equilibrium intermetallic beta initially present. Another defect is inverse segregation wherein there exists macrosegregation, (concentration gradient) with higher magnesium and zirconium content on the outside of the casting. This develops during direct chill casting wherein solute rich liquid flows toward the surface through interdendritic channels.

#### B. ROLLING

During rolling, edge cracking and development of residual stresses are potential problems. These may have a large effect on both strength and ductility of the material. During rolling, inhomogeneous deformation in the through-thickness direction can cause edge cracking. If the material on the surface of the billet is worked more than that in the interior there will be residual stresses introduced. The residual stresses result in the exterior of the billet being in compression and the interior being in tension. This is the result of light reductions during rolling and the effect can be visually observed on the edges of the billet as "overhanging" material after rolling is complete. Heavy reductions during rolling can cause the opposite effect when the center of the billet, in the thickness direction, expands

laterally more than the surface, to produce barrelled edges. Another defect is alligatoring, a type of fracture which is caused by either a metallurgical weakness enhanced by an improper balance of stresses in the billet or by a curling effect if one roll is higher or lower than the centerline of the roll gap [Ref. 9]. During ambient temperature tension testing, if residual stresses exist within the microstructure of the specimen, internal cracking may initiate in conjunction with these residual stresses, causing premature failure and thus reducing the ductility.

### C. MICROSTRUCTURAL CHARACTERISTICS

#### 1. Microstructure at Ambient Temperature

Superplastic microstructures should also be excellent microstructures for ambient temperature mechanical properties. The microstructural prerequisites for superplasticity include: 1) fine, equiaxed grain structures with high angle grain boundaries; 2) a second phase present in finely distributed form of size usually near  $1.0\text{ }\mu\text{m}$ ; 3) a thermally stable microstructure. Wert [Ref. 10] has discussed the importance of precipitate particle size for grain refinement and grain coarsening control in high strength aluminum alloys. Particle diameter of less than  $1\text{ }\mu\text{m}$  suppresses discontinuous nucleation and retards growth of recrystallized grains, while particles greater than  $1\text{ }\mu\text{m}$  in size create nucleation sites for recrystallized grains. During the warm rolling process dislocation density is increased. Having a fine dispersion of a second phase particles combined with a high dislocation

density promotes a fine recrystallized grain size. Wert [Ref. 10] concludes that extensive deformation in the warm rolling process with a duplex alloy provides an equiaxed microstructure.

## 2. Strengthening Mechanisms

Grain size refinement is not normally considered to confer significant strengthening in Al alloys. However, Gurland [Ref. 11] has reviewed data on Al-Si alloys and suggests that a 1.0  $\mu\text{m}$  grain size may contribute 140 MPa to the yield strength. Such refined grain size has been reported in an Al-Mg-Mn alloy by McNelley, Lee and Mills, and Lee, McNelley and Stengel [Ref. 12, 13].

## D. SUPERPLASTIC BEHAVIOR

Superplasticity is the ability of a material to deform to at least two hundred percent tensile elongation without fracture. In addition to the prerequisites stated in the previous paragraph, the prerequisites for superplasticity also include: 1) high strain rate sensitivity; 2) elevated temperatures in the range of 0.5 to 0.7  $T_m$ ; 3) low strain rates; 4) resistance to cavitation [Ref. 14].

Superplastic behavior is found in materials in which flow stress is highly strain rate sensitive. In analysis of deformation at elevated temperatures, the flow stress  $\sigma$  is related to strain rate by a power law relationship, equation 2.1:

$$\sigma = K\dot{\epsilon}^m \quad (\text{eqn 2.1})$$

where  $K$  is a temperature-dependent material constant and  $m$  is the strain rate sensitivity coefficient. The coefficient  $m$  may also be defined as equation 2.2:

$$m = \frac{d(\ln \sigma)}{d(\ln \dot{\epsilon})} \quad (\text{eqn 2.2})$$

This would be the slope of a stress versus strain rate plot of logarithmic axes of experimental data. The  $m$ -value for superplastic materials usually ranges from 0.3 to 0.7. As  $m$  increases, resistance to necking increases and consequently greater ductility results [Ref. 15].

Numerous models are presented in the literature to explain the deformation mechanisms involved in superplasticity. Sherby and Ruano [Ref. 16] report an equation which most closely reflects the mechanisms observed in the aluminum-magnesium alloys of this research:

$$\dot{\epsilon} = (K_1 \frac{D_{eff}}{E^{1/m}}) \frac{1}{d^p} \sigma^{\frac{1}{m}} + K_2 D_s \sigma^3 \quad (\text{eqn. 2.3})$$

Equation 2.3 states that the total strain rate  $\dot{\epsilon}$  is the sum of that due to a superplastic mechanism (the first term on the right hand side) and that of a dislocation creep mechanism.  $K_1$  and  $K_2$  are material constants,  $D_{eff}$  is the effective diffusion coefficient,  $D_s$  is the solute diffusion coefficient,  $d$  is the mean grain diameter,  $\sigma$  is the flow stress,  $m$  is the strain rate sensitivity coefficient, and  $p$  is the grain size exponent. Using equation 2.3 as a

model for superplasticity in these Al-Mg alloys, a stable grain size will facilitate the determination of the true  $m$  value. At high strain rates and high stresses, there will be a transition to the dislocation creep mechanism of the second term on the right hand side. If the grain size is unstable, i.e., growth occurs with time and strain, then application of equation 2.2 to experimental data will not reveal the true  $m$  suggested in equation 2.3 but rather a lesser value.

#### E. WHY THE PRESENT WORK

##### 1. Purpose

Extensive research has been conducted at the Naval Postgraduate School on the high magnesium alloy Al-10%Mg-0.1%Zr.

Alcamo [Ref. 17] studied the effects of the Zirconium addition to high magnesium alloys. Concurrently, Berthold and Hartman [Ref. 18, 19] concentrated on microstructural aspects and mechanical testing at various temperatures, respectively. They concluded that superplasticity was readily attainable in Al-10%Mg-0.1%Zr. Klankowski [Ref. 7] concentrated on the ambient temperature service properties after simulated superplastic forming of various alloys including Al-10%Mg-0.1%Zr. He concluded that strength was retained but ductility varied from 1 to 14 percent. Future application of such alloys will require ductility at the upper end of such a range and understanding of the cause of lower ductility.



## 2. Approach

The principal focus of this research was on the ambient temperature ductility. Initial efforts attempted to reproduce previous thesis work in order to study both testing procedures and the thermomechanical process (TMP) itself. Through the use of light microscopy (LM) and scanning electron microscopy (SEM), the microstructure was observed and changes made in the TMP procedure to improve both strength and ductility. Ambient and elevated temperature (300°) tension testing was conducted to study the effect of processing changes. .



### III. EXPERIMENTAL PROCEDURE

#### A. MATERIAL

The aluminum alloy investigated contained nominally 10%Mg and 0.1%Zr (wt. %). The direct-chill cast ingot was produced by ALCOA Technical Center using 99.99% pure aluminum base metal alloyed with commercially pure magnesium, Al-Zr master alloy, Ti-B addition for grain size control in the as-cast condition, and Beryllium as 5% Be Aluminum-Beryllium master alloy for oxidation control [Ref. 20]. The as-received ingot measured 127 mm (5 in) in diameter and 1016 mm (44 in) in length. Table I lists the complete chemical composition of the alloy examined [Ref. 20].

TABLE I

ALLOY COMPOSITION (WEIGHT PERCENT)

Serial Number	Si	Fe	Mg	Zn	Al
572826	0.02	0.02	9.90	0.09	Bal.

#### B. PROCESSING

Processing followed the sequence shown in Figure 3.1. The ingot was sectioned into billets 95.3 mm (3.75 in) long with a square cross section 31.8 mm (1.25 in) square. Following the procedure developed by Johnson [Ref. 2], and refined by Becker [Ref. 21], the billets were solution treated above the solvus, at 440°C for 5 hours and then at 480°C for 19 hours. The billet surface temperatures were

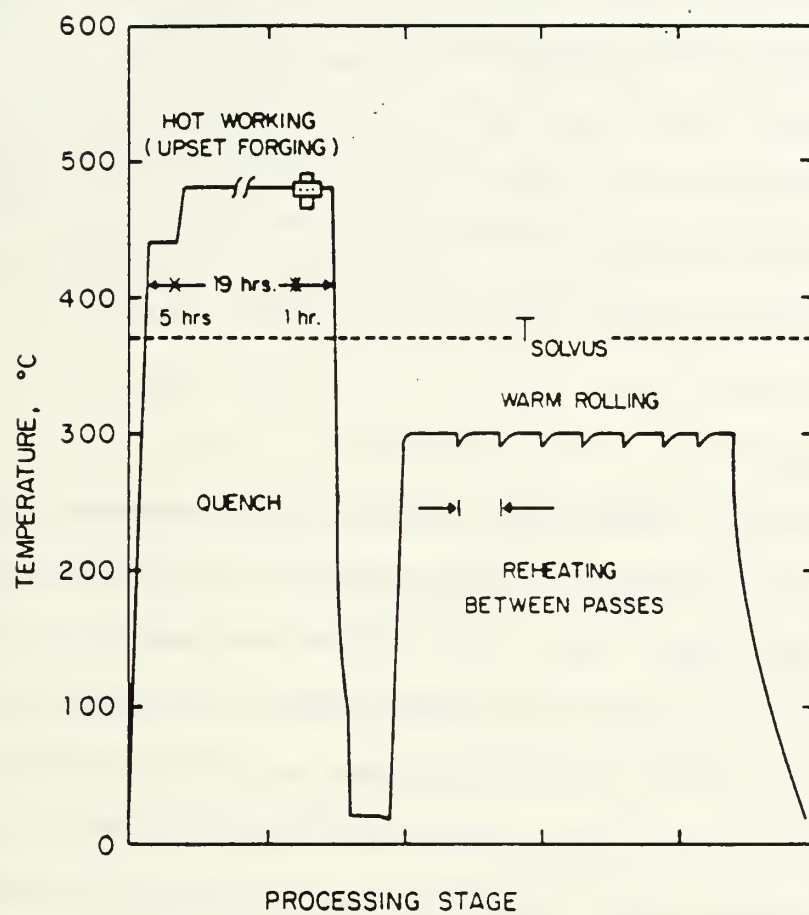


Figure 3.1. Schematic of the thermomechanical processing technique.

monitored with two thermocouples. Then the billets were upset forged at 480°C on heated platens to approximately 25.4 mm (1 in) in height. Subsequently, they were resolution treated at 480°C for 1 hour, and vigorously oil quenched. The billets were forged longitudinally, resulting in a reduction of approximately 71% for a true strain of 1.3. To improve the homogeneity of the microstructure, some billets were upset forged to approximately 20.3 mm (0.8 in) in height. This resulted in a reduction of approximately 78% for a true strain of 1.5.

#### C. WARM ROLLING

The billets were then warm rolled within 24 hours of upset forging into sheets in accordance with the technique reported by Mills [Ref. 22]. The billet was heated to 300°C for 30 minutes to achieve isothermal conditions prior to the first rolling pass. This was done to prevent cracking of forged billets due to uneven heating during the rolling process. To achieve the isothermal condition the billets were placed two at a time on a large steel plate, which acted as a heat sink in a preheated furnace. The billet surface and steel plate temperatures were monitored using three thermocouples. The billets were then rolled in accordance with the reheat time and thickness reduction schedule used by Klankowski [Ref. 7, p. 24] which now will be referred to as the light reduction schedule. Final reduction during such rolling was approximately 89% equivalent

to a true strain 2.2. For a heavy reduction scheme during rolling, the billets were divided equally in two parts and rolled with the roll separation decrease by 2.0 mm (0.08 in) per pass to achieve a final average sheet thickness of 3.1 mm (0.12 in). This resulted in a reduction of approximately 85% for a true strain of 1.9. Between each successive pass the sheet was returned to the furnace for four minutes to maintain isothermal conditions. To reduce bowing, the rolled sheet was rotated endwise after each pass, always maintaining the initial longitudinal direction. The rolled sheets were then cut into blanks, maintaining the rolling direction as the longitudinal dimension for the blanks. Specimens for ambient temperature testing were machined to the dimension presented by Klankowski [Ref. 7, p. 27] for ambient temperature test specimens. Specimens used in elevated temperature testing conformed to the dimensions established by Becker [Ref. 21]. Machining of test specimens was as described by Hartman [Ref. 19]. Special attention was given to ensure blanks were cut in longitudinal directions and any stress concentrations or burrs were removed. This was done out of concern for possible notch sensitivity resulting from processing or a material defect.

#### D. AMBIENT AND ELEVATED TEMPERATURE TESTING

Ambient temperature testing was conducted on an electro-mechanical Instron machine. The Instron machine was calibrated before each series of tests. Specimens were mounted in both

screw type grips and in wedge action grips. A crosshead speed of 1.27 mm/min (0.05 in/min) was used for all ambient temperature testing. This provided a strain rate of  $8.33 \times 10^{-4} \text{ s}^{-1}$  for the 1 inch gage section. Specimens tested were in the as-rolled condition and also after annealing at 300°C for 0.5, 1, 2, 5, and 10 hours. Elevated temperature testing was conducted at 300°C using the Marshall model 2232 three-zone clamshell furnace. Again, the electromechanical Instron machine was calibrated before each series of tests. The equipment set up and test procedure was similar to that described by Alcamo [Ref. 17] with the exception of using five instead of three thermocouples to monitor temperature gradients within the furnace. The two extra thermocouples were placed at the upper and lower pull rod screw mounts. Testing would commence once all five thermocouples were stabilized and the three thermocouples touching the test specimen were within  $\pm$  one degree centigrade. It would usually take about one hour to reach this equilibrium point. The crosshead speed ranged from 0.05 mm/min (.002 in/min) to 127 mm/min (5.0 in/min). The range of strain rates tested varied from  $6.67 \times 10^{-5} \text{ s}^{-1}$  to  $1.67 \times 10^{-1} \text{ s}^{-1}$ . Specimens tested were in the as-rolled condition and also annealing at various temperatures and times. The annealing temperatures and times were: (1) 200°C annealed for 1.0 hour; (2) 200°C annealed for 10 hours and ; (3) 300°C annealed for 1.0 hour.



## E. DATA REDUCTION

Elongation was determined by measuring the marked gage section before and after testing. Percent elongation was determined by taking the difference between the two quantities and dividing by initial gage length. The Instron strip chart recorded the applied load (lbs.) versus the chart motion. The magnification ratio for the ambient temperature testing was 40 while for the elevated temperature test the magnification ratio was 10 or 100. From the strip chart, raw data points of chart displacement and load were taken and put in data files to be reduced. A "floating slope" was used on the strip chart from which measurements were taken. This was used to remove such variables as grip adjustment and elasticity of the sample as well as Instron components themselves. This input data was analyzed by a Basic computer program, provided in Appendix B which was run on a Sanyo 555B computer. This reduced data was then sent to the IBM 3033 computer for further generation of graphics using the Easyplot routine.

## F. METALLOGRAPHY

Both optical and scanning electron microscopy were carried out in support of this research. The specimens examined included ones from various stages of processing, as well as selected samples fractured in ambient temperature testing. Specimens examined by light microscopy were first cold mounted in a cylindrical plastic medium by an acrylic



compound. Mounted specimens were then polished by wet silicon carbide abrasive paper following a sequence of 240, 320, 400 and 600 grit papers. This process took no longer than 20 to 30 minutes. After washing the specimen was given a rough polish on 600 grit alumina ( $\text{Al}_2\text{O}_3$ ) powder in distilled water using billiard cloth fixed to rotating wheel at 350 RPM. For best results in the rough polishing considerable hand pressure should be used initially and then be gradually reduced. This process took a maximum of three minutes to complete. After the rough polishing, an ultrasonic cleaning was necessary to remove any embedded abrasive particles before final polishing. The final polishing was accomplished with an eleven micron magnesium oxide powder ( $\text{MgO}$ ). For best results, a teaspoon of the abrasive should be applied to the center of a nap cloth moistened with distilled water. Then, add enough distilled water so that after mixing of the abrasive a thick paste is created. Finally, with moderate to light pressure, polish the specimen adding distilled water as necessary to maintain abrasive consistency [Ref. 23]. All optical micrographs of specimens examined in the solution treated condition (before the rolling process) were obtained after electropolishing at  $20^\circ\text{C}$  with a mixture of methanol and 20 percent  $\text{HNO}_3$  for 10 seconds at 10 volts d.c. The specimens were then electroetched using Keller's reagent (2 ml HF, 3 ml HCL, 5 ml  $\text{HNO}_3$ , 190 ml  $\text{H}_2\text{O}$ ) for 15-20 seconds at 20 volts d.c. For those specimens examined after the rolling, the electropolishing solution was reduced to  $0^\circ\text{C}$  by

liquid nitrogen and polishing took 1/2 second at 10 volts d.c. The electroetching took 1-2 seconds at 10 volts d.c. All electroetching was conducted at ambient temperature. Before any optical examinations were conducted, the electropolishing solution was rinsed in a beaker filled with methanol and the specimen was then dried. For the electropolish specimens were rinsed in a fresh water beaker and then dried. Metallographic examination was conducted with the ZEISS ICM 405 optical microscope and A CAMBRIDGE STEREOSCAN 200 scanning electron microscope.

## IV. RESULTS

### A. METALLOGRAPHIC CHARACTERIZATION

#### 1. As-Cast Microstructure

The Al-10%Mg-0.1%Zr alloy used in this research was produced by the direct chill cast method. This is described in further detail by Berthold [Ref. 18, p. 35]; the direct chill casting method provides a relatively high cooling rate which is necessary to minimize coring and segregation in semicontinuous production of large volumes of material.

Light microscopic study of the as-cast material shows dendrite formation and eutectic thus demonstrating the non-equilibrium structure produced by the casting process. Berthold [Ref. 18, p. 36] demonstrated by energy dispersive analysis that  $\text{ZrAl}_3$  forms as a primary phase in the direct chill casting. Pashley [Ref. 24], working with Al-6%Cu-0.5%Zr, concluded that an important requirement was a uniform, fine distribution of  $\text{ZrAl}_3$ . It is desired to dissolve all the zirconium in the melt and to retain it in solution until after solidification of the alloy. If this cannot be accomplished, then coarse primary  $\text{ZrAl}_3$  particles will form as a result of the peritectic in the Al-Zr system and these will not contribute to grain refinement and the superplastic properties of the alloy.

## 2. Solution-Treated Microstructure

Solution treatment was done at 480°C following an initial heating at 440°C; the initial heating was intended to dissolve the non-equilibrium eutectic to avoid hot shortness. Figure 4.1(a) shows an SEM micrograph of Al-10%Mg-0.1%Zr alloy which was solution treated for 5 hours at 440°C, 19 hours at 480°C and then vigorously oil quenched. The specimen was obtained from a section one centimeter from the ingot's outer surface as illustrated in Figure 4.2. The dendrite structure observed in the as-cast condition is still present. Figure 4.1(b) using the SEM back scattering mode, demonstrates the lighter areas indicate a lesser atomic weight. This suggests a high concentration of Mg near the surface and is indicative of inverse segregation. This inverse segregation of magnesium may result in brittleness in further processing treatments if insufficient surface is removed.

## 3. Upset Forged Condition

Figure 4.3(a) shows the microstructure of a billet which was given a reduction of 78% equivalent to a true strain of 1.5 in upset forging. This structure is slightly coarser than that reported by Becker [Ref. 21], who conducted solution treatment at 440°C only. Also, a lesser reduction was utilized in that previous work. The micrograph shows an equiaxed grain structure after the hot working. In hot working, the higher the temperature the coarser the grain size as recovery and recrystallization are diffusion-controlled processes [Ref. 9].



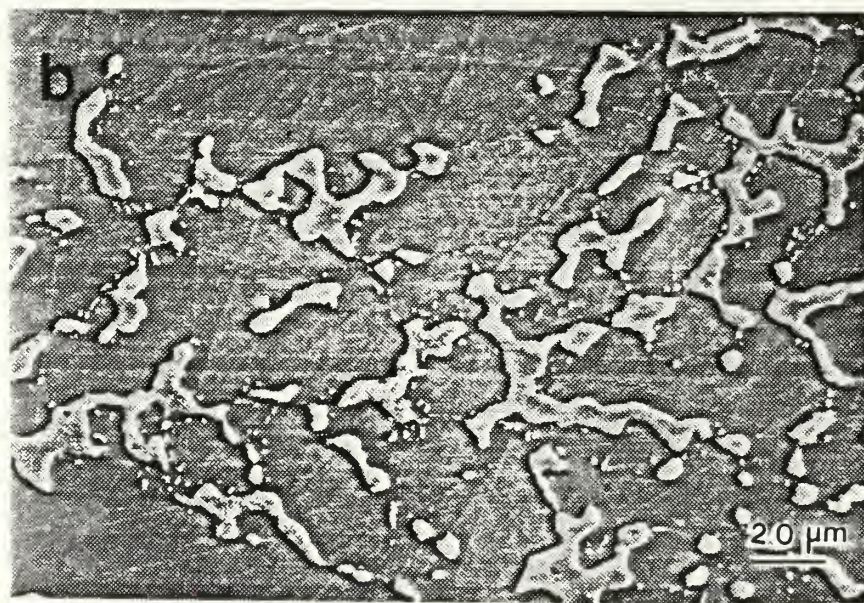
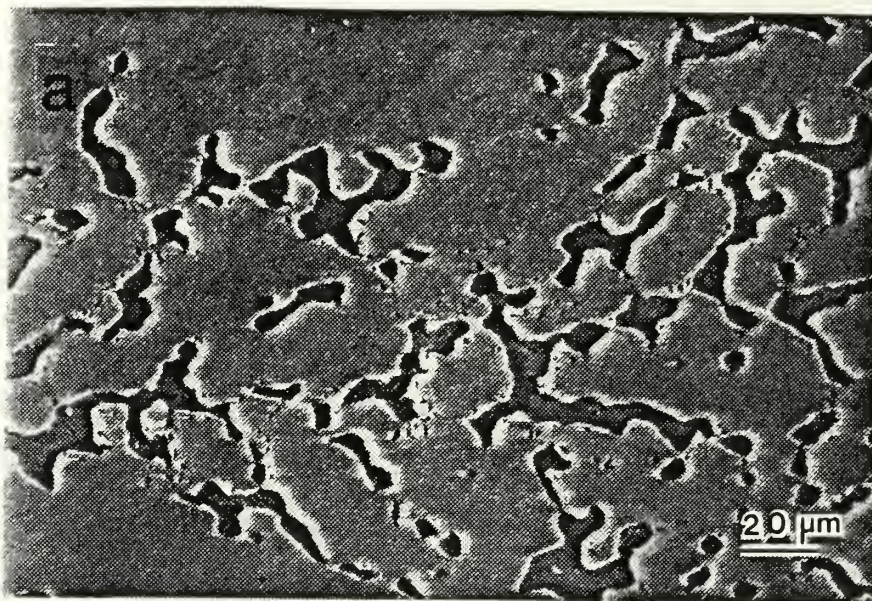
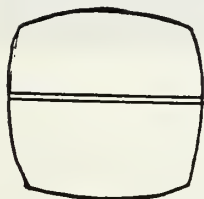


Figure 4.1. SEM micrographs of an Al-10%Mg-0.1%Zr alloy, solution treated for 5 hrs at 440°C and then 19 hrs. at 480°C. Specimen is located 1.0 cm. from ingot's outer surface;

- (a) dendritic solidification in secondary electron imaging mode;
- (b) back scattering mode reveals many  $\text{Mg}_5\text{Al}_8$ , (white particles) and a few  $\text{ZrAl}_3$ , (black particles)

TOP VIEW



SIDE VIEW



UPSET FORGE SPECIMEN

sectioning required for  
figure 4-3

a



b



Figure 4.2. Schematic illustrating sectioning for metallographic examination.



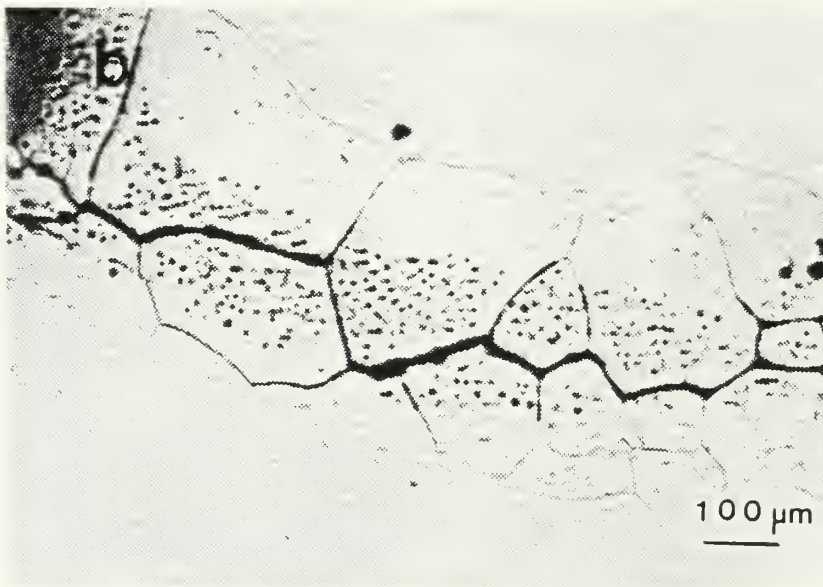


Figure 4.3. Optical micrographs of an Al-10%Mg-0.1%Zr alloy solution treated, upset forged and oil quenched: (a) under cross polarized light showing equiaxed grain structure and homogeneous dispersion of second phase; (b) bright field micrograph at outer edge of upset forged; the specimen showing intergranular cracking caused by inverse segregation.

Also seen is alignment of second phase particles, likely  $\text{ZrAl}_3$ .

After upset forging, cracking was observed on the periphery of the billet at a location near the original cast surface. Figure 4.2 shows a schematic of the sectioning required to examine a specimen after upset forging. Light microscopy Figure 4.3(b) clearly shows intergranular cracking caused by inverse segregation. Figure 4.4 provides a view of the intergranular crack under cross polarized light. Also seen is a zone of refined grains below the original surface; this likely results from inverse segregations of the  $\text{ZrAl}_3$ .

#### 4. Warm Rolled Condition

As described previously, an examination of both light and heavy rolling reduction material was conducted. Figure 4.5 shows two triplanar views of a light reduction rolled material, warm rolled at  $300^\circ\text{C}$  to a reduction of 89 percent. Figure 4.5(a) is from the center section of the rolled specimen and is inhomogeneous with the original grain structure still evident. Figure 4.5(b) is a section taken near the surface of the same rolled specimen and showing more and coarser beta but also a more uniform dispersion. The material near the surface has seen more warm working than in the center. If the working of the material is not uniform, then residual stresses will occur along with the possible edge cracking, as discussed by Dieter [Ref. 9]. Figure 4.6 shows such a defect created by the light rolling reduction. The micrograph reveals



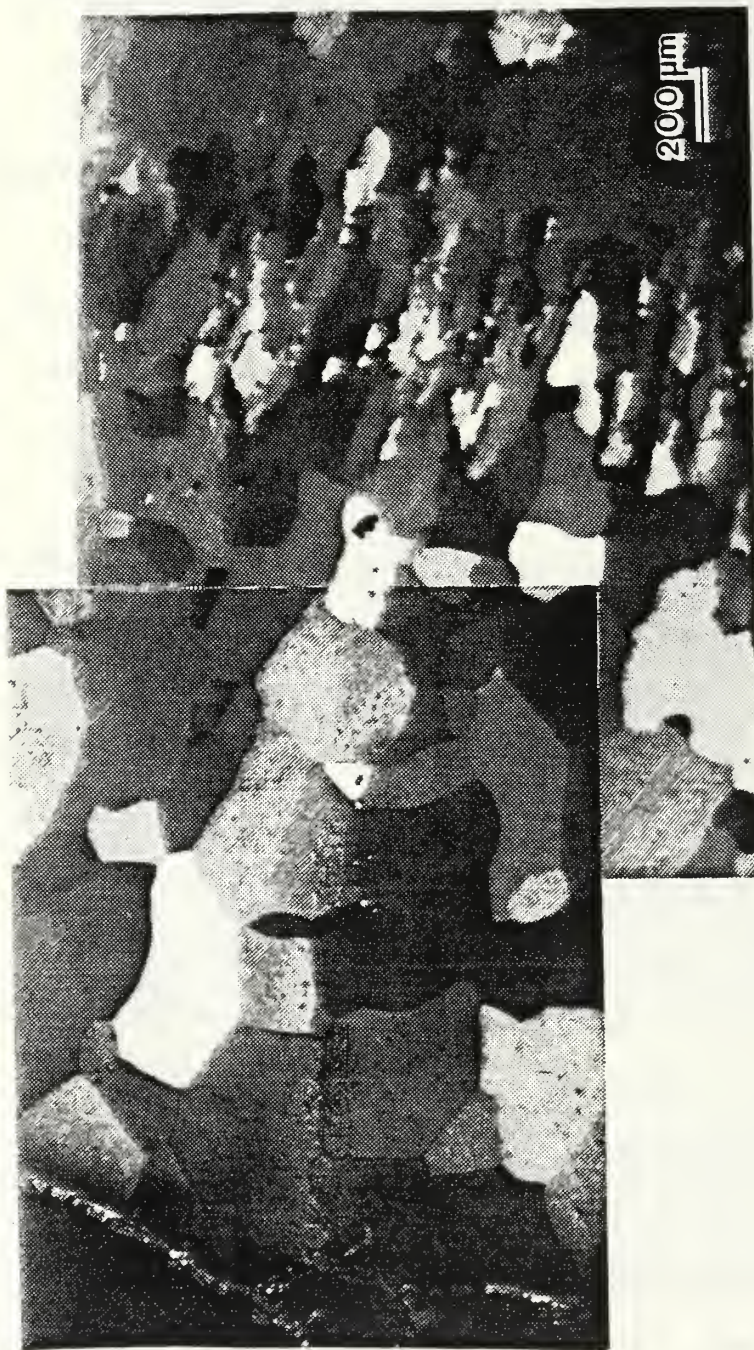


Figure 4.4. Optical micrograph of Al-10Mg-0.1Zr alloy solution treated, upset forged and oil quenched. An intergranular crack initiated on outer edge of the specimen is shown. Also seen is a region of finger grain structure, likely a result of inverse segregation of Zr.

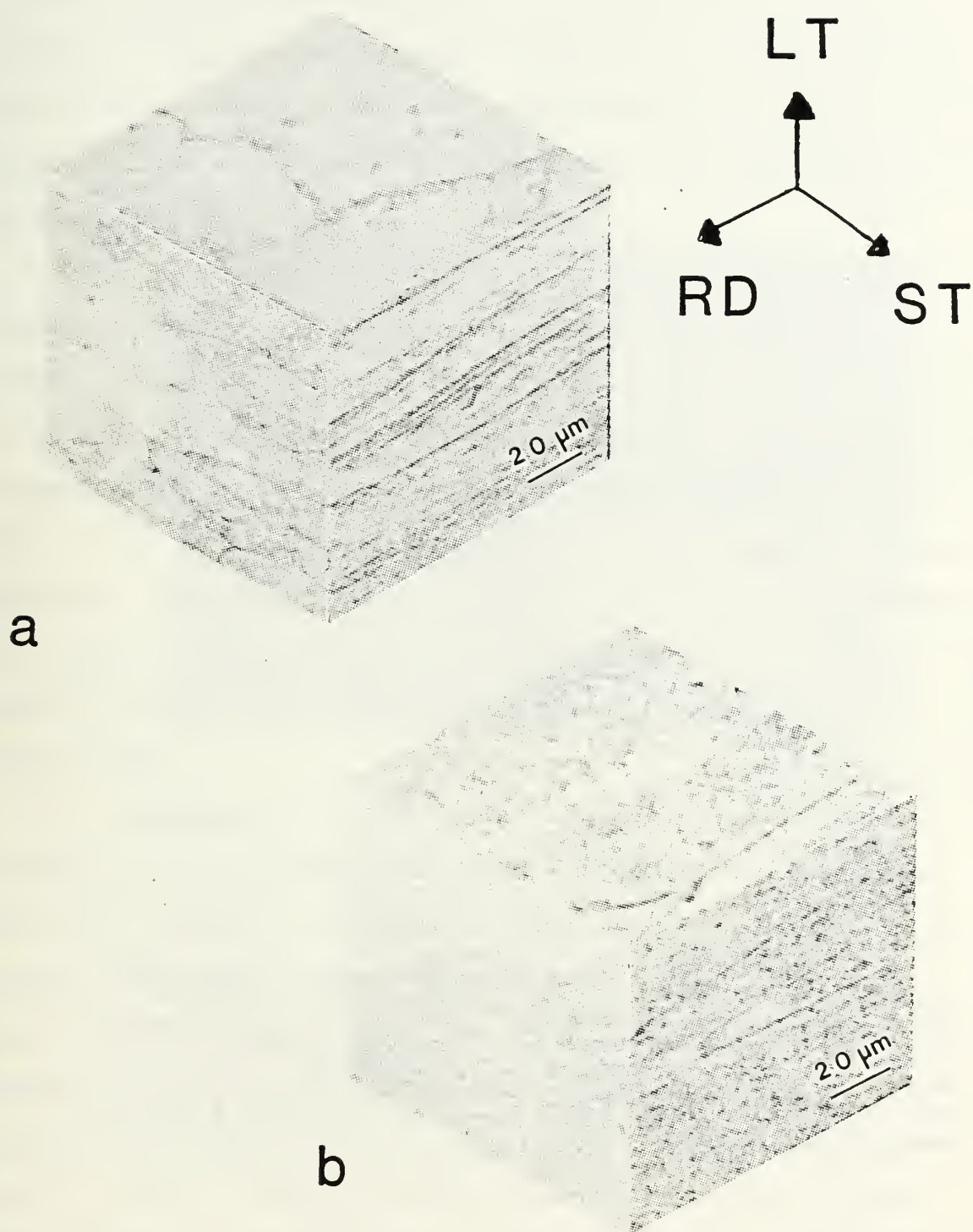


Figure 4.5. Tri-planar micrographs of an Al-10%Mg-0.1%Zr alloy warm rolled at 300°C to a true strain of 2.2 (39 percent reduction); (a) center of rolled specimen, (b) outer edge of rolled specimen.



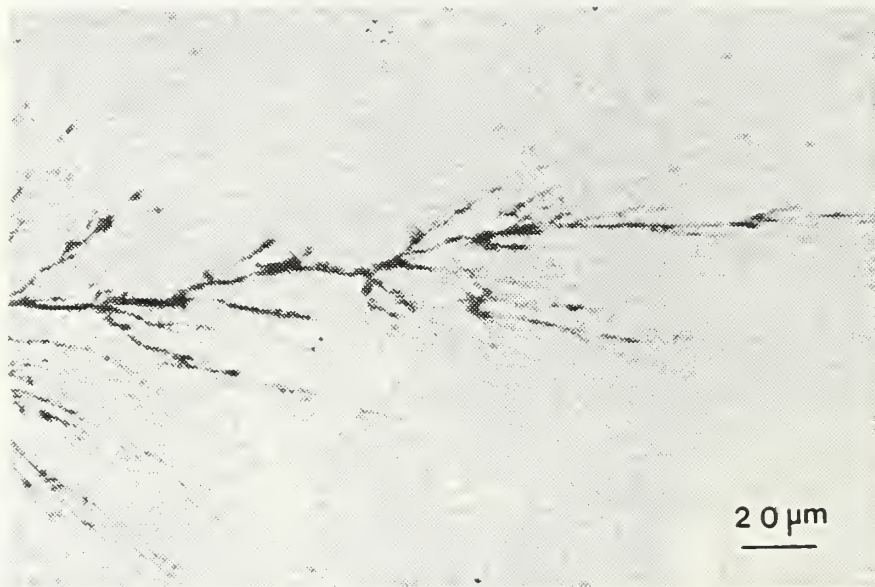


Figure 4.6. Optical micrograph of an Al-10%Mg-0.1%Zr alloy warm rolled at 300°C to 89 percent reduction utilizing light reduction in rolling. Inverse segregation coupled with low rolling reduction facilitated edge cracking, resulting in transgranular cracking, especially in regions near the original cast surface.

a transgranular crack extending 2.5 millimeters into the interior of the rolled specimen. Residual stress caused by low rolling reduction combined with inverse segregation noted in the as-cast ingot, appears to be an important factor in promoting edge cracking.

As discussed earlier, a change was made in the warm rolling process to eliminate the edge defects. By taking a bigger reduction per pass, from 1.0 mm. (0.04 in) to 2.0 mm. (0.08 in), the edge cracking was eliminated. Light microscopy investigation reveals a significant change in the microstructure. Figure 4.7(a), from material experiencing light rolling reduction, shows a uniform distribution of relatively coarser beta phase ( $Mg_5Al_8$ ); which the heavier rolling reduction material shows a finer beta phase which is less uniformly distributed.

Microscopic examination of materials experiencing different rolling schemes revealed significant differences. Figure 4.8 shows the rolling defects associated with a light rolling reduction. Figure 4.8(a) shows alligatoring which may result in a weak midplane in the rolled sheet [Ref. 9]. Figure 4.8(b) an "hour-glass" shape along the edge of the billet resulting from light reduction. In contrast, Figure 4.9 (a) and (b) reveal that with heavier reduction, these edge defects are eliminated. Uniform working of the material and diminished residual stresses result.



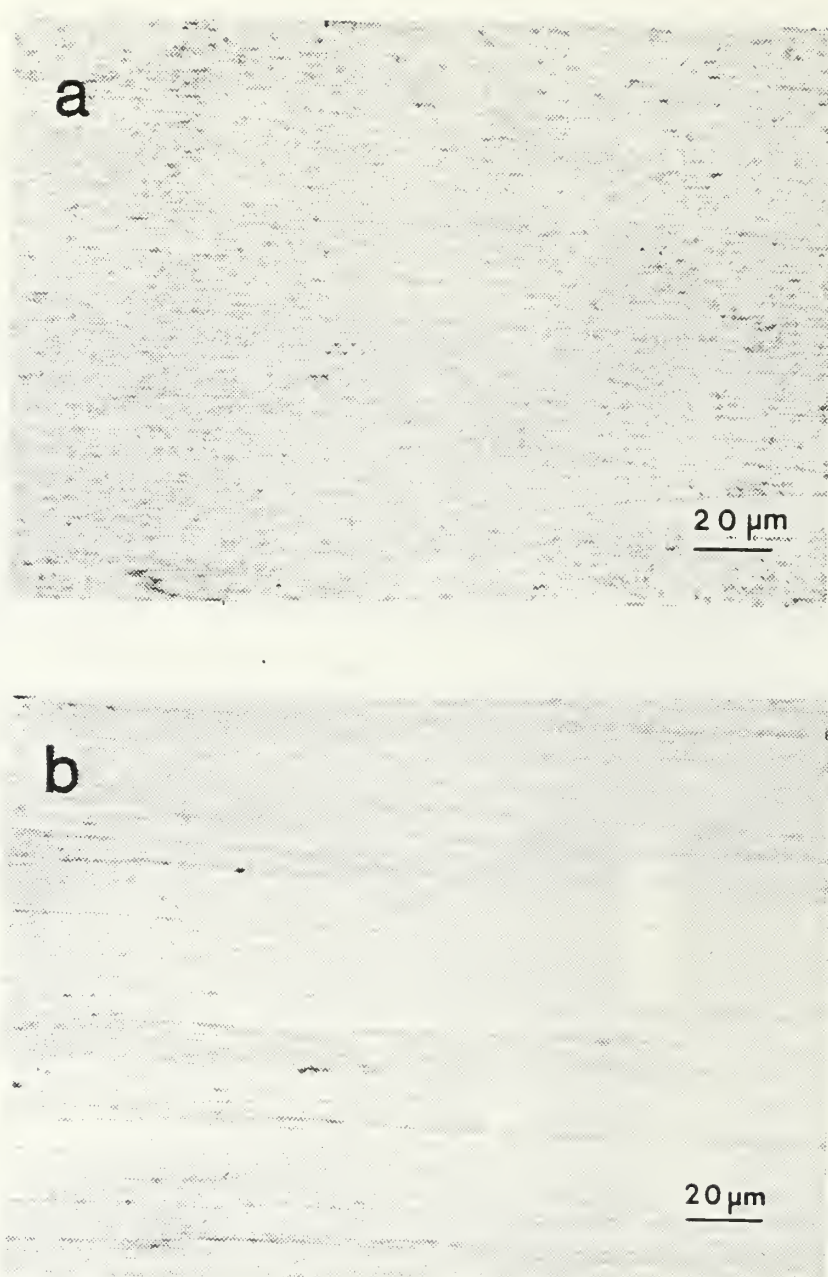


Figure 4.7. Optical micrographs of warm rolled Al-10%Mg-0.1%Zr alloy, tensile tested at ambient temperature; (a) light reduction showing fine, uniform distribution of second phase, (b) heavy reduction specimen, finer second phase, but less uniform distribution of beta phase.



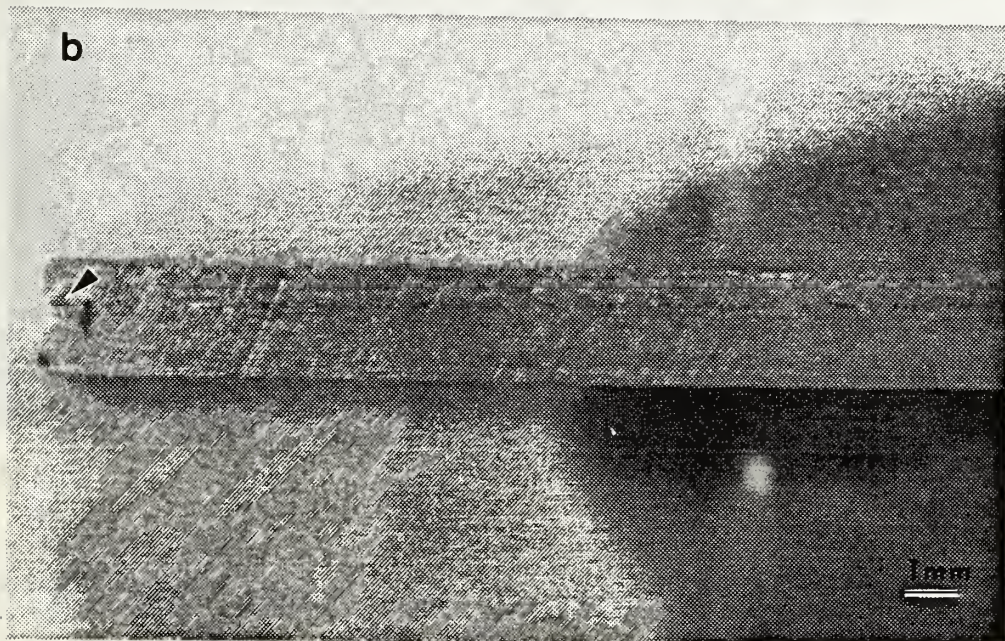
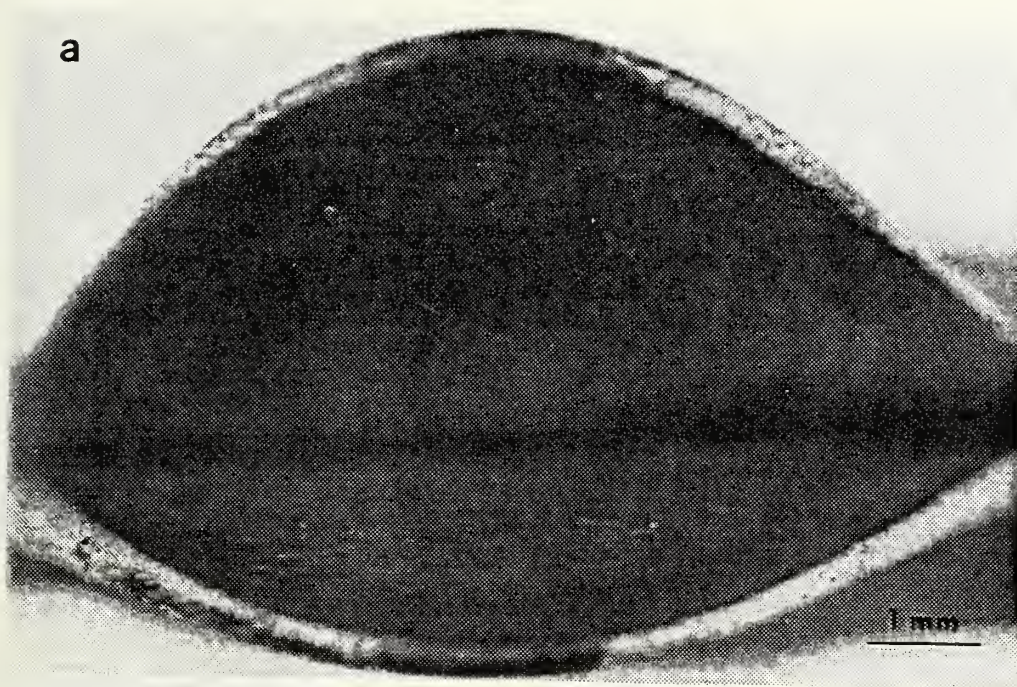


Figure 4.8. Photographs of 300°C warm rolled specimens showing (a) alligatoring due to light reduction during processing and (b) edge of same sample revealing non-uniform working of material.



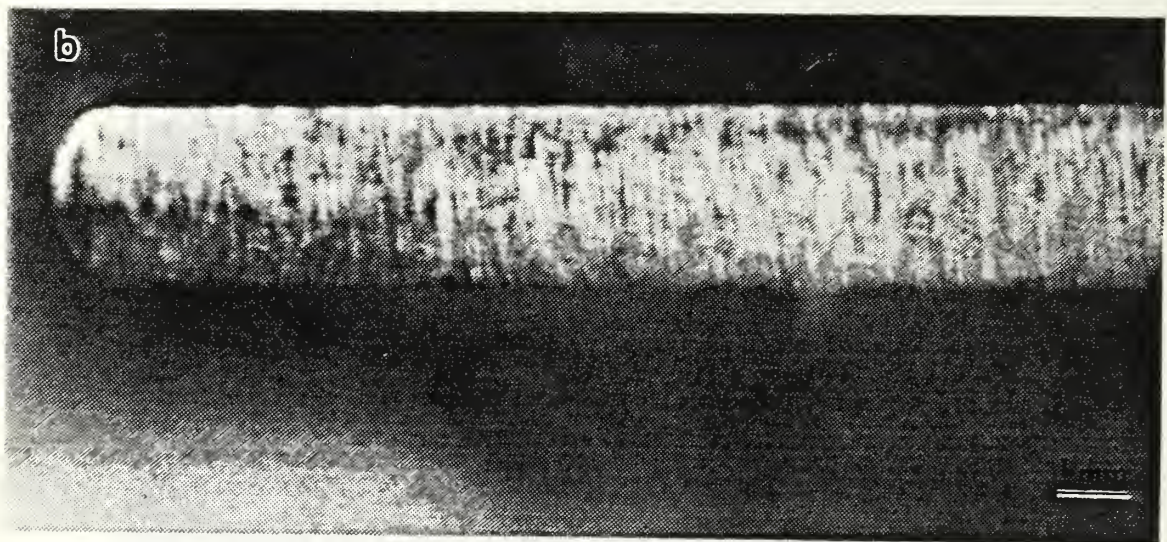
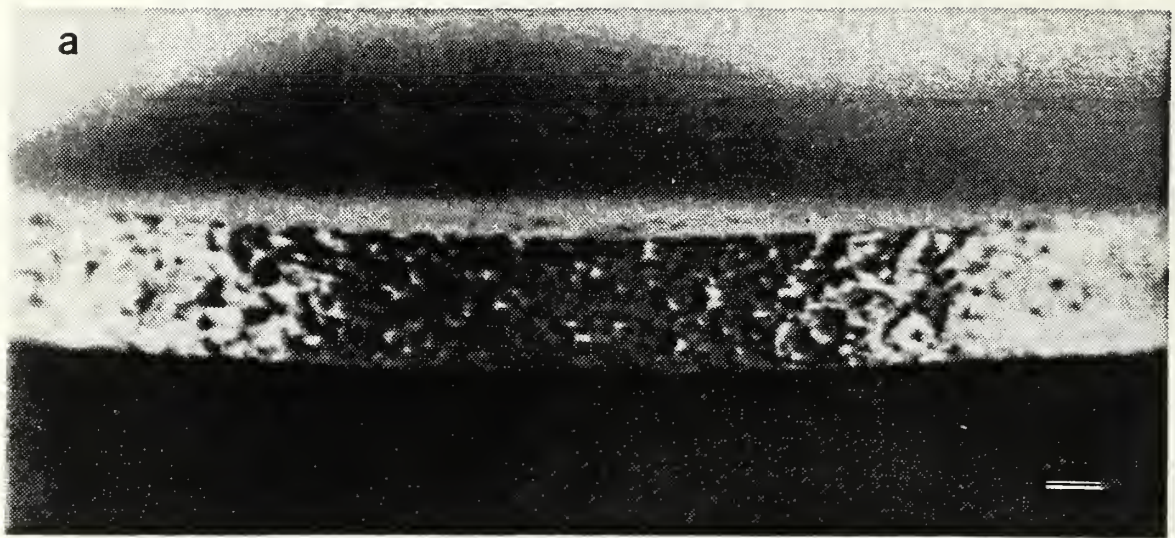


Figure 4.9. Photographs of 300°C warm rolled specimens showing (a) elimination of alligatoring in heavy reduction material and (b) uniform working of material typical of heavy reduction.

## B. MECHANICAL TESTING

### 1. Ambient Temperature Testing

The intent of the first series of ambient-temperature tension tests was to reproduce previous work, in order to ascertain if a problem existed with the testing procedure or in the TMP process and which in turn caused the variability in ductility. Following the procedure for processing, as described in Chapter III, material was rolled using the light reduction scheme reported by Klankowski [Ref. 7]. Specimens were tested in the as-rolled condition and following various 300°C anneals times, (data provided in Table III). Figure 4.10(a) shows that in the as-rolled condition, ductility is approximately 8 percent. After one-half hour of annealing at 300°C, the ductility reaches 20 percent. Although annealing time was increased to 10 hours, ductility remained constant at 20 percent. Figure 4.10(b) shows that at in the as-rolled condition, yield strength was approximately 296 MPa (43 KPSI) and ultimate tensile strength was 483 MPa (70 KPSI). After annealing for one-half hour at 300°C, the yield strength decreased to 207 MPa (30 KPSI) and the ultimate tensile strength decreased to 386 MPa (56 KPSI). At longer annealing times, neither yield strength or ultimate tensile strength change more than 10 percent. Comparison with Klankowski's data [Ref. 7, p. 39] reveals very similar results. In the second series of ambient-temperature tension tests, tighter tolerances were imposed in the milling process used to

TABLE II

AMBIENT TEMPERATURE MECHANICAL TEST DATA OF  
AL-10%MG-0.1%ZR ALLOY IN THE AS-ROLLED CONDITION  
(LIGHT REDUCTION PROCESSING) AND FOR ANNEALING  
TIMES AT 300°C.

FIRST SERIES:

TIME ANNEAL AT 300°C (HRS)	$\sigma_Y$		$\sigma_\mu$		PERCENT STRAIN MEASURE (%)
	(KPSI)	(MPA)	(KPSI)	(MPA)	
0	42.3	291.3	68.5	472.2	8.0
0	44.6	307.5	72.8	501.9	10.0
0.5	28.8	198.5	54.8	377.8	20.8
0.5	26.6	183.4	55.4	381.9	19.5
1.0	29.1	200.7	56.5	389.5	19.0
1.0	30.7	211.6	57.5	396.4	16.0
2.0	27.2	180.3	55.5	382.6	21.8
2.0	28.5	196.5	59.60	390.22	20.0
5.0	29.5	203.3	52.9	364.7	18.0
10.0	27.8	191.6	55.9	385.3	20.3

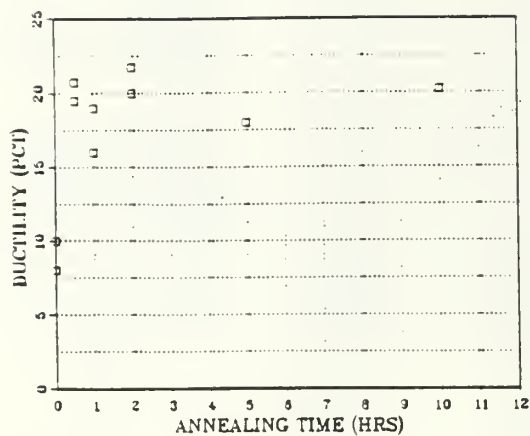
SECOND SERIES

TIME ANNEAL AT 300°C (HRS)	$\sigma_Y$		$\sigma_\mu$		PERCENT STRAIN MEASURE (%)
	(KPSI)	(MPA)	(KPSI)	(MPA)	
0	58.4	402.6	75.6	521.2	6.5
0	45.2	311.6	70.8	488.1	6
0	52.2	359.8	71.1	490.2	13.4
0	63.6	438.5	75.3	519.1	6.5
0.5	40.0	275.8	62.6	431.6	16.5
0.5	43.7	301.28	59.5	410.2	12.0
0.5	38.8	267.5	67.8	467.4	13.0
0.5	37.8	260.6	60.8	419.2	14.5
0.5	35.6	245.4	60.3	415.2	15.5
1.0	49.8	343.3	75.2	518.5	16.8
1.0	44.5	306.8	64.3	443.3	16.3
1.0	40.7	280.6	62.2	428.8	18.0
1.0	37.9	261.3	60.9	419.9	19.0

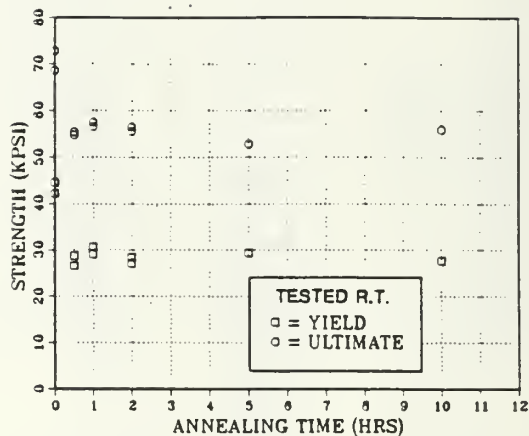


TABLE II (CONT'D)

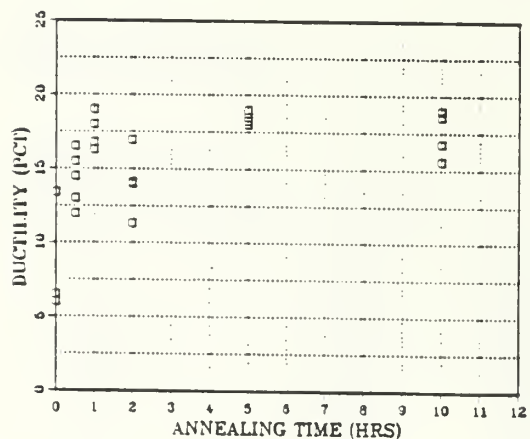
TIME ANNEAL AT 300 C (HRS)	$\sigma_Y$		$\sigma_\mu$		PERCENT STRAIN MEASURE
	(KPSI)	(MPA)	KPSI)	(MPA)	(%)
2.0	38.6	266.1	61.7	425.4	14.12
2.0	40.2	277.1	59.6	410.9	11.4
2.0	36.8	253.7	60.8	419.2	17.0
2.0	47.2	290.9	58.8	405.3	14.0
5.0	35.2	242.6	60.0	413.6	18.0
5.0	33.6	231.6	59.2	358.5	18.5
5.0	37.6	259.2	61.9	426.7	19.0
5.0	36.5	251.6	60.5	417.1	18.3
10.0	34.1	235.0	59.0	406.7	18.6
10.0	34.2	235.7	60.3	415.8	19.0
10.0	31.8	219.2	57.4	395.7	16.8
10.0	32.8	226.1	58.8	405.4	15.6



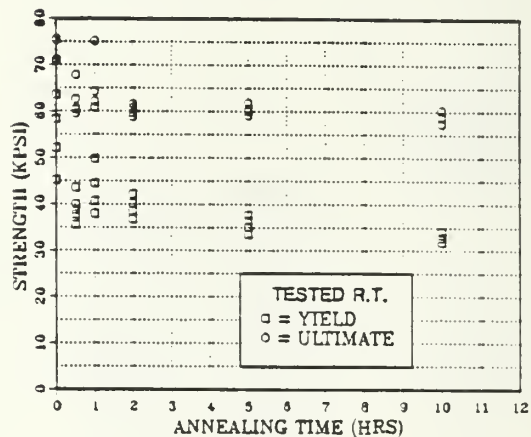
a



b



c



d

Figure 4.10. Results of ambient temperature tension testing of material processed as in previous work; (a) and (b) are the results of the first series of tests, while (c) and (d) are the second series of tests.

fabricate test specimens. This was done to evaluate specimen geometry. The use of wedge action grips instead of the screw type grips was also introduced to minimize slippage. Figures 4.10 (c) and (d) and data provided in Table II show similar results to the first series of tension testing, leading to the conclusion that specimen geometry is not a cause for variability in ductility.

For the final series of ambient-temperature tension tests, the material was processed differently. First a larger reduction was taken in the upset forging process. Then, the material was more heavily rolled in the warm rolling process; the true strain attained in rolling was 2.0. Data provided in Table III and Figure 4.11(a) shows the as-rolled condition ductility to be increased to approximately 18 percent, compared with the light rolling 300°C for 5 hours, the ductility increased slightly to 20 percent. Figure 4.11 (b) shows in the as-rolled condition, the heavy rolled material has comparable yield strength and slightly lower ultimate tensile strength. As annealing at 300°C increases to 5 hours, yield strength decreases to approximately 225 MPa (32.5 KPSI) and ultimate tensile strength decreases to approximately 386 MPa (56 KPSI). This is comparable to the yield and ultimate strengths obtained after annealing in the first two series of tests. Figure 4.12 shows stress versus strain curves which compare typical data for a lightly versus heavily rolled material. The lighter rolled material shows

TABLE III

AMBIENT TEMPERATURE MECHANICAL TEST DATA OF  
Al-10%Mg-0.1%Zr ALLOY IN THE AS-ROLLED  
CONDITION (HEAVY REDUCTION PROCESSING) AND  
FOR VARIOUS ANNEALING TIMES AT 300°C

TIME ANNEAL AT 300°C (HRS)	$\sigma_y$		$\sigma_\mu$		PERCENT STRAIN MEASURE (%)
	(KPSI)	(MPA)	(KPSI)	(MPA)	
0	48.6	335.0	67.8	467.4	19.5
0	58.6	404.0	74.2	511.5	19.3
0	51.1	352.3	65.0	448.1	19.0
0	47.9	330.2	63.3	436.4	17.5
0	49.7	342.6	66.3	457.1	19
0	50.4	347.5	66.7	459.8	18.5
1.0	37.3	257.2	60.5	417.1	15.0
1.0	39.4	271.6	58.9	406.1	16.5
1.0	34.8	239.9	58.2	401.2	18.5
1.0	357.0	246.1	58.0	399.9	16.0
5.0	31.7	218.5	57.9	399.2	17.0
5.0	32.8	226.1	55.3	381.3	16.5
5.0	31.1	214.4	56.0	386.1	19.5
5.0	33.1	228.2	56.7	390.9	20.5
5.0	34.0	234.4	57.4	395.7	19.0

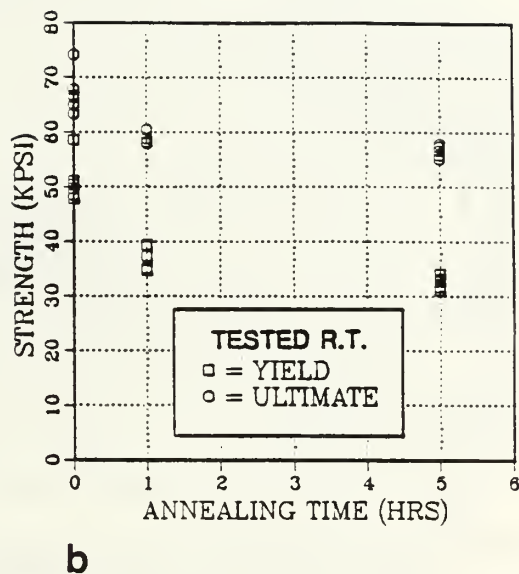
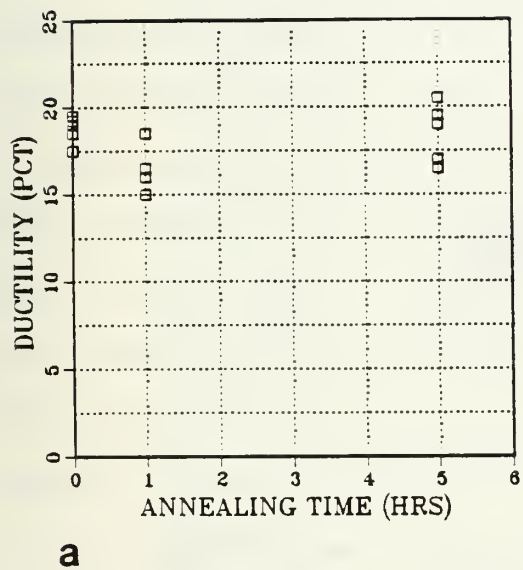


Figure 4.11. Results of ambient temperature tension testing of heavy reduction processed material; (a) and (b) are the results of the third series of tests.



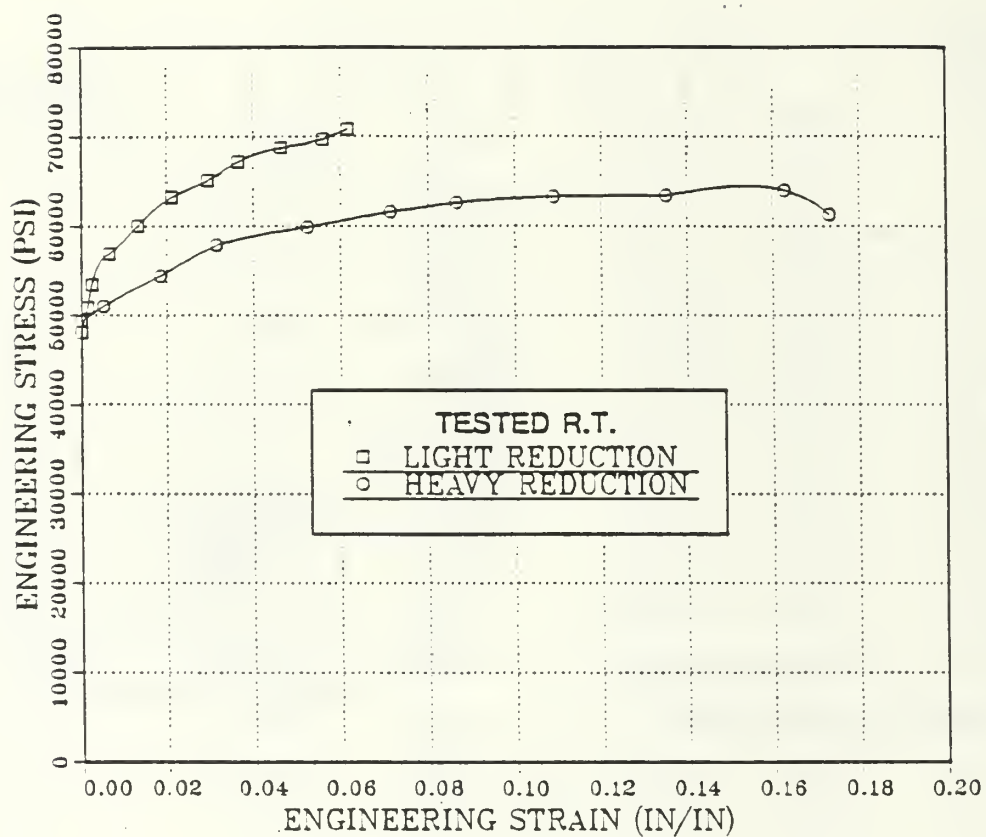


Figure 4.12. Engineering stress versus engineering strain for an ambient temperature tension test on as-rolled material showing a comparison between heavy and light reduction processing of material.

higher strength. Recalling that after annealing in the first two series of tests, the ductility increased from 8 to 20 percent and noting that annealing produces strain free grains, it may be concluded that residual stresses in lighter rolled reduction material lead to premature failure in the as-rolled specimens at ambient temperature.

Examination of the fracture surface after ambient temperature tension tests was done by the use of scanning electron microscopy. Figure 4.13 (a) shows fractography of a light rolled reduction specimen with 6 percent ductility. The fracture surface is V-shaped, shiny on the sides and dull in the middle. Figure 4.13 (b) is a higher magnification view of the center section of the fracture surface. The crack observed here is one of many found near the center regions of the fracture. The cracks are all parallel to the rolling direction. Further investigation by light microscopy and SEM revealed that these cracks are only observed on the surface of the fracture. This suggests again the conclusion that these internal cracks are a result of residual stresses accumulated during the rolling process. Figure 4.13 (c) shows a fine, equiaxed dimple pattern. Figure 4.14 (a) shows the fractography of a heavy rolled reduction specimen with 19 percent ductility. The fracture surface is shiny and inclined at 45 degrees to the tensile axis. Higher magnification views, Figure 4.14 (b) and (c), show a transgranular failure with more ductile tearing and elongated dimples. Ashland [Ref. 1]



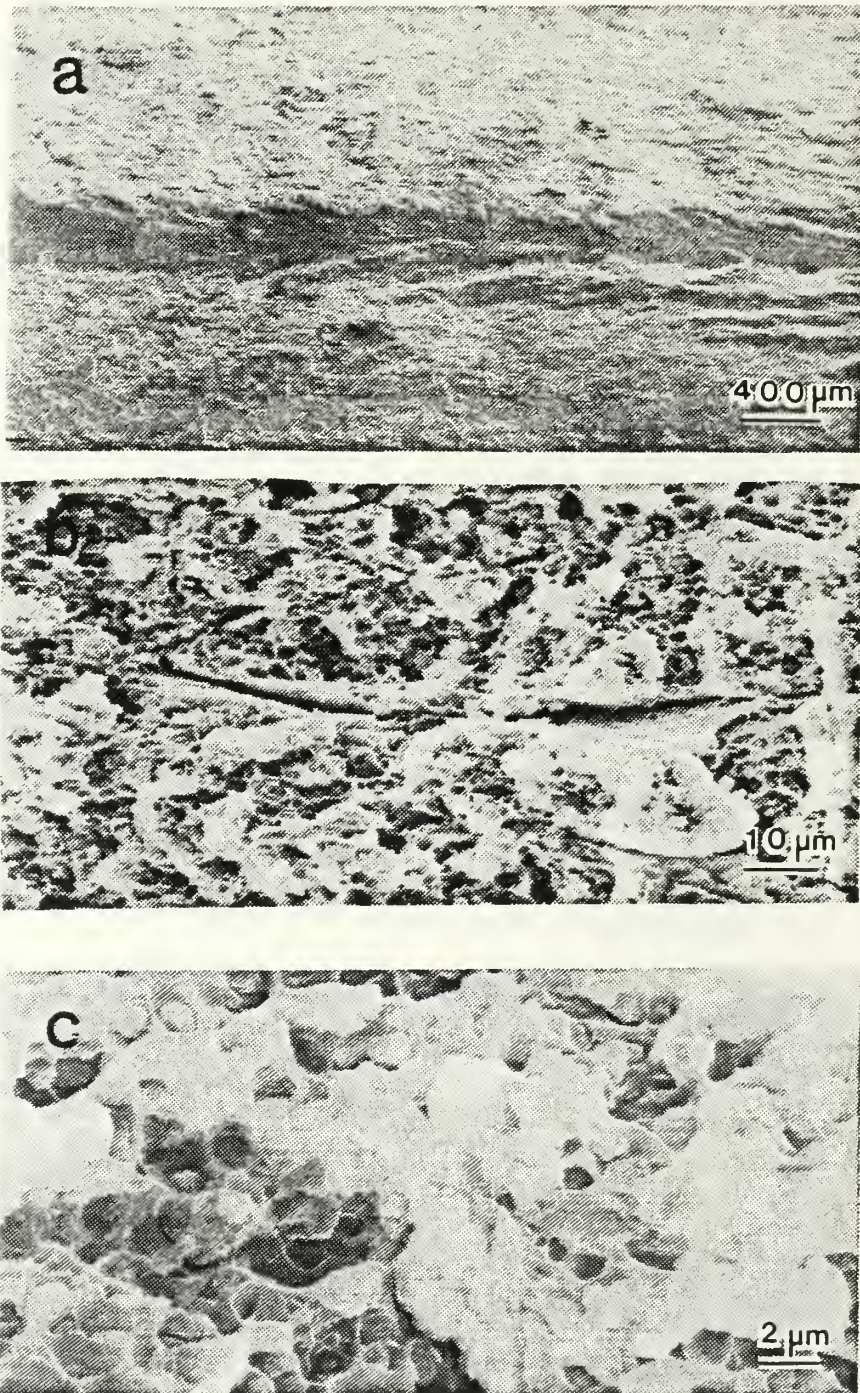


Figure 4.13. SEM micrographs of a test specimen tension tested at ambient temperature following light reduction processing. Ductility was 6.0 percent elongation to fracture; fracture surface at (a) 24X, (b) 1000X, (c) 4000X.



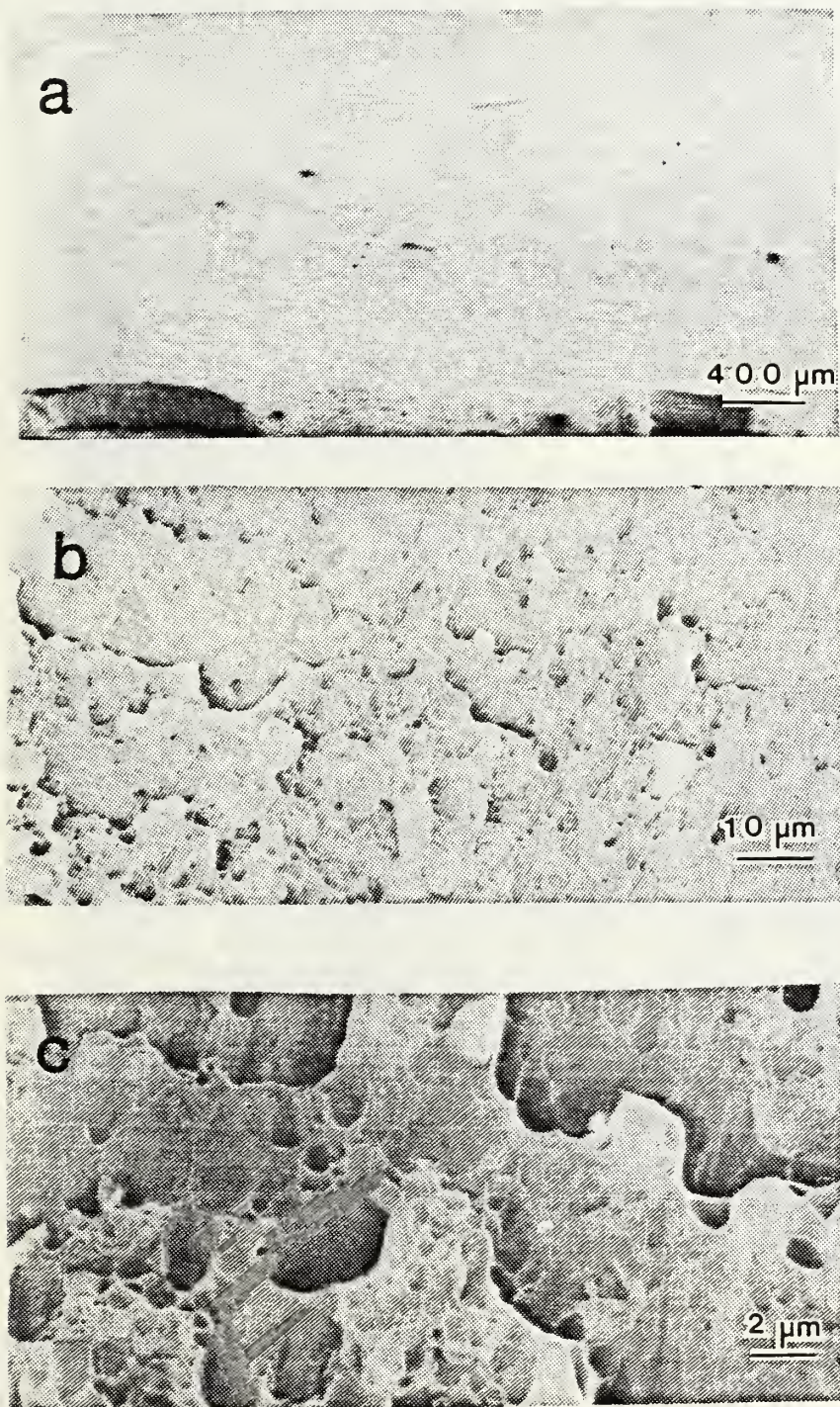


Figure 4.14. SEM micrographs of a test specimen tension tested at ambient temperature following heavy reduction processing. Ductility was 19.0 percent elongation to fracture; fracture surface: (a) 26.5X, (b) 1000X, (c) 4000X.

describes these elongated dimples as a suggestive of soft inclusions or second phase particles present in the matrix. Figure 4.15 (a) is at high magnification of the light rolled material, revealing an intermetallic beta particle ( $Mg_5Al_8$ ) approximately  $1.25\text{ }\mu\text{m}$  in size. Figure 4.15 (b) is also at high magnification of the heavy rolled material, which revealed no second phase particles, evidence of a finer, softer second phase. Due to time constraints in testing, the heavier rolled material was not given simulated superplastic forming and subsequent ambient temperature testing as was done in Klankowski's work [Ref. 7].

## 2. Elevated Temperature Testing

### a. Stress - Strain Response

This part of the investigation was conducted to study the deformation characteristics of the light versus heavy rolled reduction material at elevated temperature; materials were studied both in the as-rolled and annealed conditions. As described in Chapter III, elevated temperature tension testing was conducted at  $300^\circ\text{C}$ . The three annealing conditions for those materials annealed prior to testing were: (1)  $200^\circ\text{C}$  for one hour, (2)  $200^\circ\text{C}$  for ten hours and (3)  $300^\circ\text{C}$  for one hour. The strain rates employed varied from  $6.67 \times 10^{-5}\text{ s}^{-1}$  to  $1.67 \times 10^{-1}\text{ s}^{-1}$ .

Typical stress strain data for a series of tension tests on as-rolled material are provided in Figure 4.16 (a) as engineering stress versus engineering strain and Figure 4.16(b)



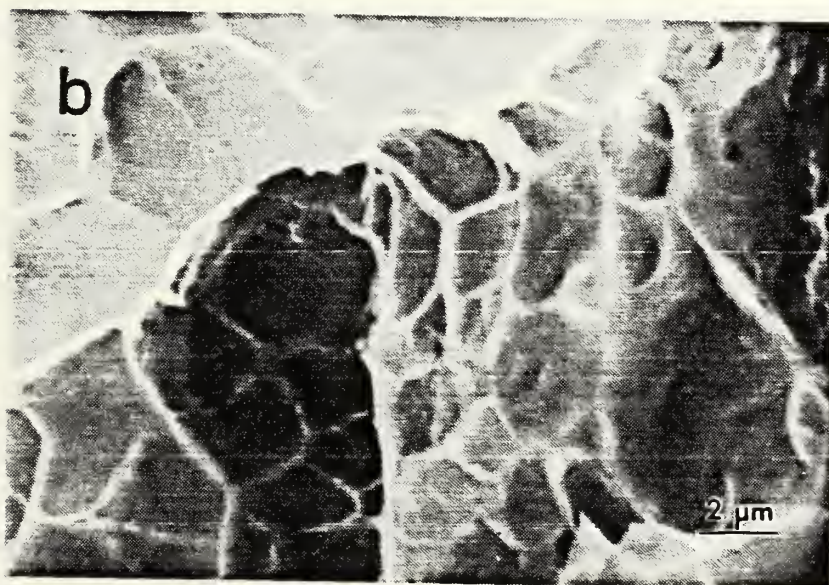
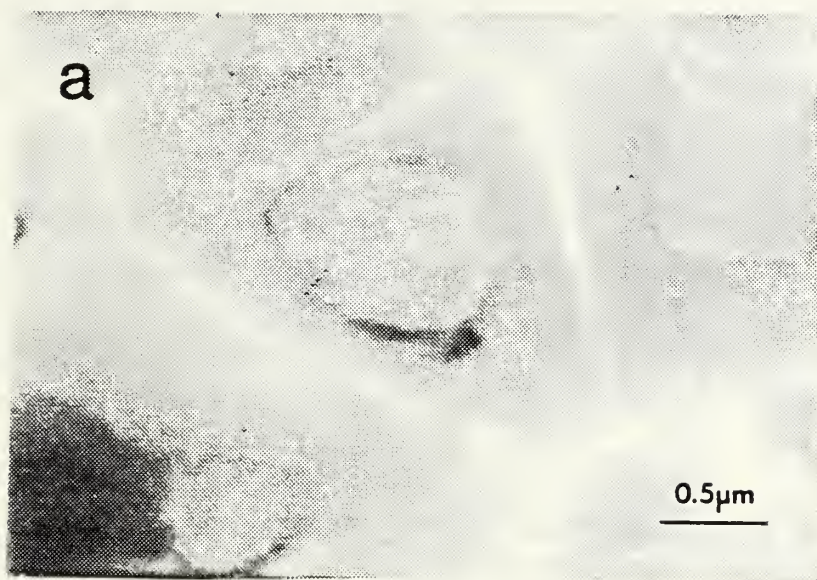
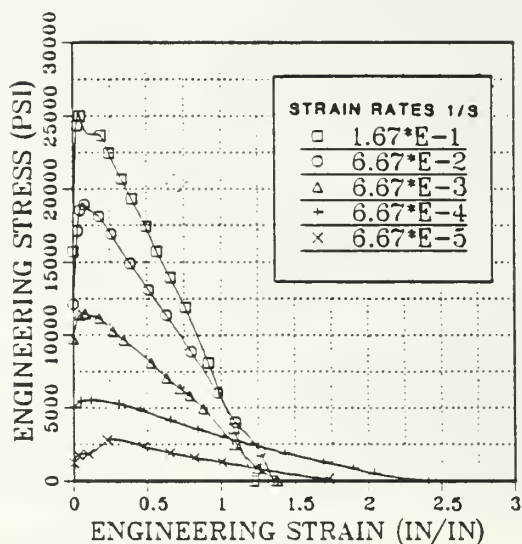
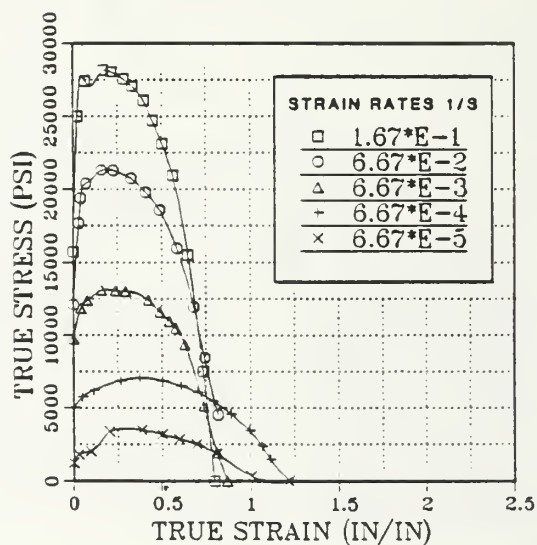


Figure 4.15. SEM micrographs of test specimen tension tested at ambient temperature; (a) light reduction specimen showing a one micron beta particle in a dimple, (b) heavy reduction specimen showing no visible beta particles associated with dimples on the fracture surface.



a



b

Figure 4.16. Tension testing conducted at 300°C for Al-10%Mg-0.1%Zr warm rolled at 85 percent reduction using heavy reduction processing of the material; (a) engineering stress versus engineering strain; (b) true stress versus true strain.

as true stress versus true strain. Data for the remainder of the test conditions are provided in Appendix A. Beyond the maximum strength, the true stress-true strain is not meaningful due to the onset of necking. These curves exhibit prolonged necking during deformation, a common characteristic of superplastic materials. Figure 4.16 shows maximum elongation is attained at a strain rate of  $6.67 \times 10^{-4} \text{ s}^{-1}$  for the as-rolled and the annealed conditions. This corresponds closely to Hartman's and Alcamo's data [Ref. 19, 17] wherein strain rates of  $7 \times 10^{-3}$  to  $7 \times 10^{-4} \text{ s}^{-1}$  exhibited the greatest degree of superplasticity. Examination of Figure 4.16 reveal that the lower the strain rate, the lower the yield strength, for both as-rolled and annealed materials.

#### b. Stress - Strain Rate Data

To compare the light reduction material and the heavy reduction material, values of true stress at 0.1 strain were obtained for the various strain rates employed and these are provided in Table IV and are plotted in Figure 4.17. This facilitates evaluation of the effects of the reduction scheme used. Following a heavy reduction scheme, the material is stronger than the same alloy which was rolled to a 92 percent total reduction using a light reduction scheme. Annealing the heavy reduction material at  $200^{\circ}\text{C}$  for one hour reduces its strength but improves its superplastic ductility only slightly. The strain rate sensitivity coefficient was approximately 0.38 for all three conditions represented. Data for other annealed conditions are included in Figure A.3. (appendix).

TABLE IV

MECHANICAL TEST DATA FOR THE Al-10%Mg-0.1%Zr  
ALLOY, TESTED AT 300°C IN THE AS-ROLLED CONDITION,  
AND FOLLOWING VARIOUS ANNEALING TREATMENTS PRIOR TO  
ELEVATED TEMPERATURE TESTING.

## PREVIOUS DATA (ALCAMO)

STRAIN RATE ( $\text{SEC}^{-1}$ )	TRUE STRESS AT 0.1 TRUE STRAIN		DUCTILITY (PERCENT ELONG.)
	(KPSI)	(MPA)	
$1.67 \times 10^{-1}$	23.1	159.2	178.8
$1.67 \times 10^{-1}$	23.2	160.4	11.04
$6.67 \times 10^{-2}$	18.0	124.1	220.6
$6.67 \times 10^{-3}$	9.4	64.9	484.4
$6.67 \times 10^{-3}$	7.0	48.3	280.6
$6.67 \times 10^{-4}$	4.3	29.6	330.0
$6.67 \times 10^{-5}$	2.0	13.8	270.0

## ANNEALED 200°C 1.0 HR.

$1.67 \times 10^{-1}$	22.5	155.1	114.0
$6.67 \times 10^{-2}$	18.8	129.6	125.0
$6.67 \times 10^{-3}$	11.0	75.8	227.0
$6.67 \times 10^{-4}$	5.1	35.2	254.0
$6.67 \times 10^{-5}$	2.6	17.9	264.0

## ANNEALED 300°C 1.0 HR

$1.67 \times 10^{-1}$	22.4	154.4	138.0
$6.67 \times 10^{-2}$	19.0	130.9	164.0
$6.67 \times 10^{-3}$	12.7	87.5	250.0
$6.67 \times 10^{-4}$	7.0	48.3	280.0
$6.67 \times 10^{-5}$	3.0	20.68	290.0



TABLE IV (CONT'D)

## ANNEALED 200°C 10 HRS

$1.67 \times 10^{-1}$	21.6	148.9	130.0
$6.67 \times 10^{-2}$	19.8	136.5	162.0
$6.67 \times 10^{-3}$	11.1	76.5	250.0
$6.67 \times 10^{-4}$	6.0	41.4	284.0
$6.67 \times 10^{-5}$	3.1	21.4	262.0

## AS-ROLLED

$1.67 \times 10^{-1}$	28.3	195.1	122.0
$1.67 \times 10^{-2}$	20.6	142.0	135.0
$6.67 \times 10^{-3}$	12.7	87.6	178.0
$6.67 \times 10^{-4}$	6.3	43.4	241.0
$6.67 \times 10^{-5}$	2.8	19.3	238.0



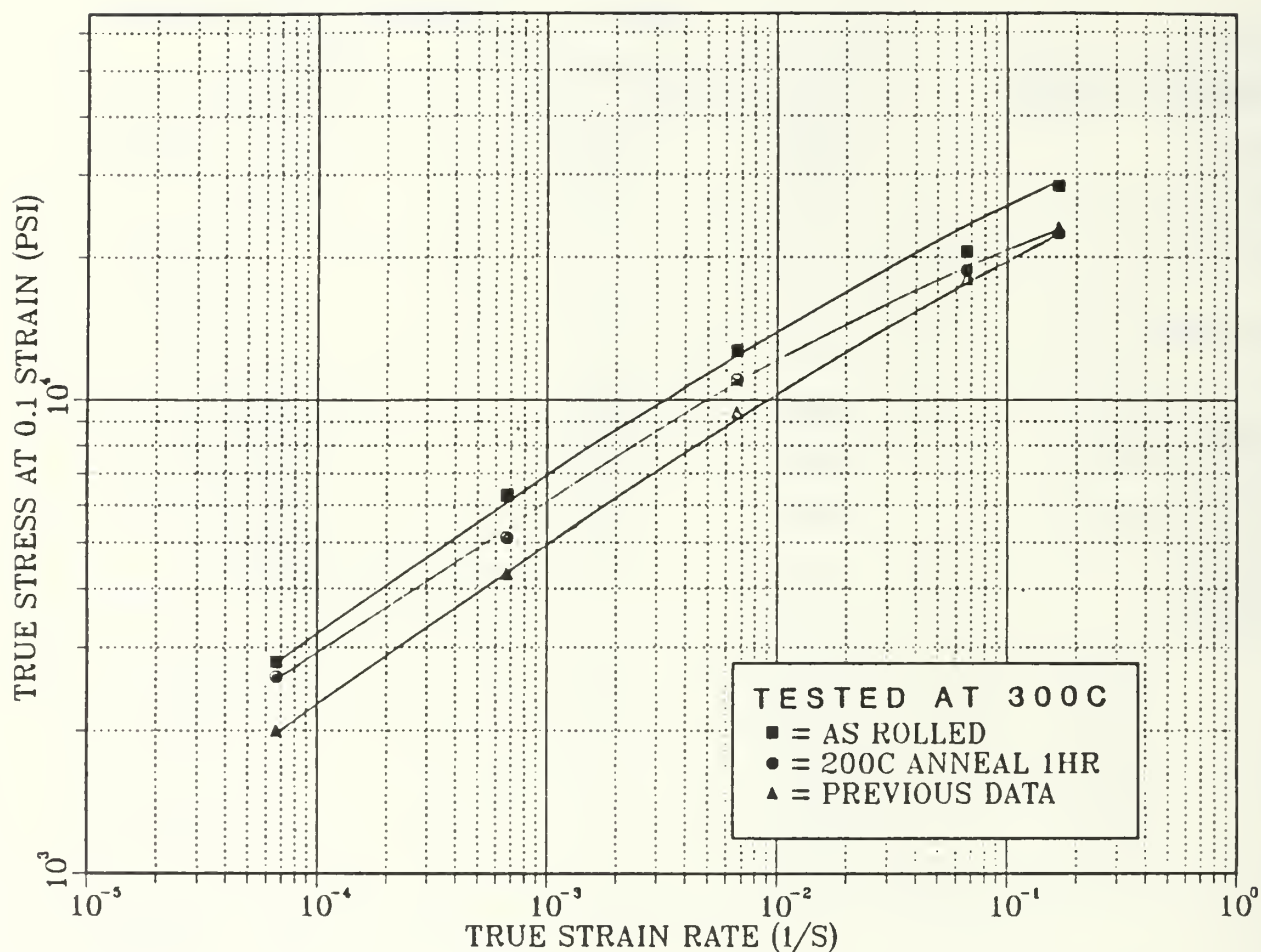


Figure 4.17. True stress at 0.1 strain versus strain rate for the Al-10%Mg-0.1%Zr alloy tension tested at 300°C. Specimens were warm rolled at 300°C to 85 percent reduction using the heavy reduction processing of material. Compare with previous data (the previous material was warm rolled at 300°C to 92 percent reduction using a light reduction scheme); the heavy reduction material was tested at various annealed temperatures and times.

c. Ductility - Strain Rate Data

Ductility data corresponding to the data of Figure 4.17 is plotted in Figure 4.18. It is seen that essentially all of the conditions evaluated in this research are less superplastic than those evaluated by Alcamo [Ref. 17]. There are two important differences in the processing prior to elevated temperature testing, namely the total rolling strain and the reduction scheme used to attain that strain.

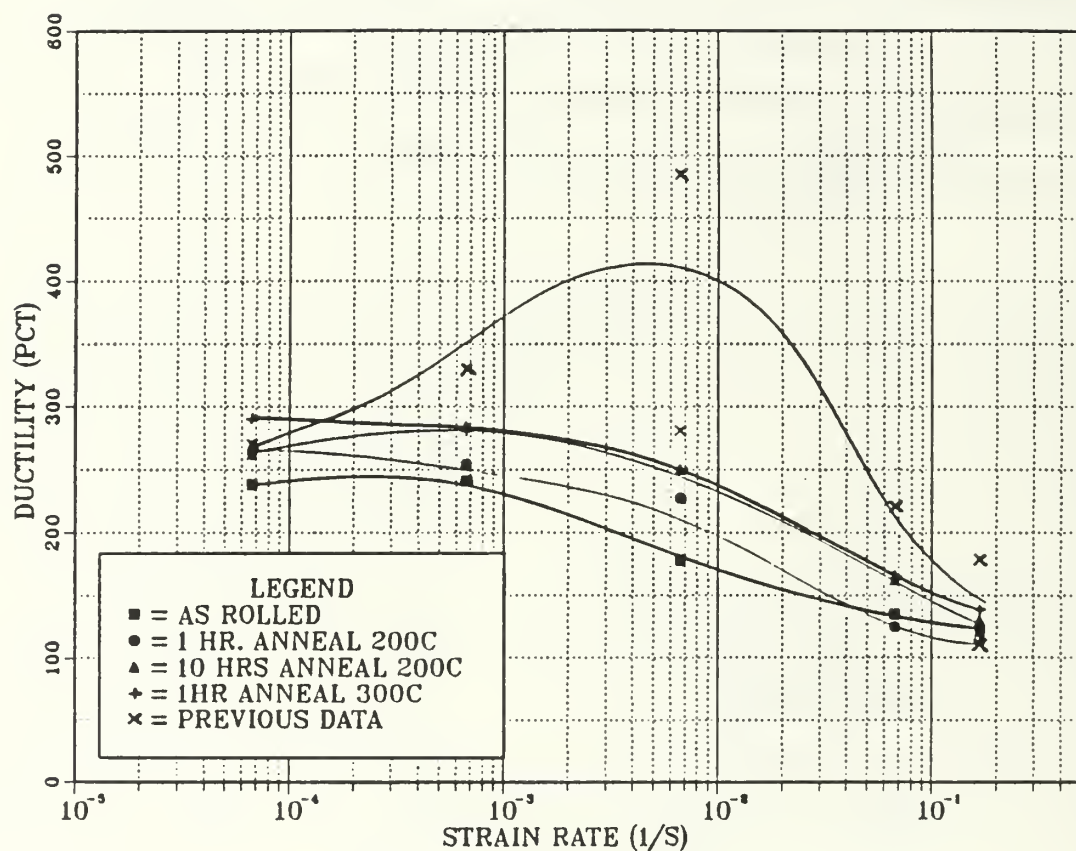


Figure 4.18. Ductility versus strain rate for tension testing conducted at 300°C on the Al-10%Mg-0.1%Zr alloy. Comparison between previous work on as-rolled light reduction processing of material warm rolled at 300°C to 92 percent reduction to a heavy reduction processing of material warm rolled at 300°C to 85 percent reduction. The heavy reduction specimens were also tested in as-rolled and at various annealing temperatures and times.

## V. DISCUSSION

### A. THE EFFECT OF ROLLING REDUCTION ON MICROSTRUCTURES

Before beginning the warm rolling sequence, the microstructure is a fine, equiaxed grain structure with magnesium in solid solution. Deforming the material produces an elongated grain structure, precipitation of intermetallic beta phase and increasing dislocation density. This is accomplished under a warm rolling temperature of 300°C, near the solvus to obtain the precipitation as well as recovery. Recovery results in formation of dislocation substructure along with excess dislocations remain in subgrain interiors [Ref. 25]. By rolling at a higher strain rate, i.e. allowing less recovery time, the microstructure should have a net increase in dislocation density and less recovery. Wert [Ref. 10] reports that if heavy deformation is not used, then the original elongated grains are not sufficiently distorted and recrystallization does not produce an equiaxed and duplex microstructure needed to enhance superplastic properties in processing of high strength - i.e. 7XXX, alloys. The use of heavier reduction here has also been shown to more uniformly work the material and reduce the effects of residual stresses and resultant edge cracking described by Dieter [Ref. 9].

## B. EFFECT OF ROLLING REDUCTION ON AMBIENT DUCTILITY

In the as-rolled condition, after heavy rolling reduction, an increased dislocation density can be assumed. This should have raised the yield strength by strain hardening effects, but experimental data reveals comparable yield strengths between light and heavy rolling reductions. In fact, the more heavier rolled material shows much higher ductility and lower strain hardening in ambient temperature testing, as seen in Figure 4.12. In examining the thermomechanical process of the light rolled reduction material, more time in the oven is given for the material to recover and recrystallize during light reduction processing. Therefore, grain size strengthening due to recrystallization might account for the lightly rolled material's similar yield strength. Another possibility for similar yield strength would be residual stresses in the lighter rolled reduction material. As explained by Dieter [Ref. 9], these residual stresses might give higher apparent strength but lower ductility due to cracking during tension testing and this was seen in Figure 4.13 (b). The effect of solid solution strengthening should be the same because in both cases the same amount of magnesium is used. During the rolling process, the strengthening mechanisms of concern are strain hardening and grain size strengthening. The effect of annealing on the heavy reduction material was small in comparison to its effect on the light reduction material. Therefore, the low ductility obtained in the light reduction material is most likely caused by residual stresses.



### C. EFFECT OF ROLLING REDUCTION ON ELONGATED TEMPERATURE DUCTILITY

Figure 4.18 suggests that the lighter rolling reduction material can attain a more fully recrystallized state at the start of a tension test and therefore a finer grain structure. In comparison, the heavier rolling reduction material may not have as fine of a grain size. It is not clear at this point whether this is the result of more annealing time during rolling or a greater total reduction during the rolling. There was insufficient time to address this problem in this research. Further research in this area will also require transmission electron microscopy to clarify the microstructural differences. Higher dislocation density, associated with the heavier rolling reduction material, would usually mean a greater driving force for recrystallization. A finer recrystallized grain structure would promote greater ductility at elevated temperatures. Just the opposite is seen with the experimental data collected. The heavier rolled material is stronger and less ductile as seen in Figure 4.18.

## VI. CONCLUSIONS AND RECOMMENDATIONS

### A. CONCLUSIONS

The following conclusions are drawn from this research.

1. After reproduction of both rolled and annealed material in accordance with established TMP procedures, ambient temperature testing revealed that testing procedures and geometry specification of specimens are satisfactory. The variability in ductility is a result of material processing.
2. Inverse segregation is present throughout the TMP process on billets taken near the outer surface of the ingot.
3. Inverse segregation and light reduction in the rolling process promoted residual stresses and edge cracking.
4. Heavier reductions during rolling eliminated edge defects and improved the as-rolled ambient temperature ductility from 8 percent to 19 percent.
5. The heavier reduction rolling resulted in a less uniformly distributed intermetallic beta phase as observed by optical and scanning electron microscope.
6. Fracture surface of higher reduction during rolling material shows a less ductile tearing and dimple formation and less or no evidence of particles in voids. This is evidence of a finer second phase.

7. Tension tests conducted at 300°C on the heavy rolling reduction material shows lower ductility in the range of strain rates of  $6.67 \times 10^{-2} \text{ s}^{-1}$  to  $6.67 \times 10^{-4} \text{ s}^{-1}$  when compared to lighter rolling reduction.

#### B. RECOMMENDATIONS

The following are recommendations for further study of the Al-10%Mg-0.1%Zr alloy.

1. Conduct a series of experiments to hold total strain constant in the rolling process and vary the mechanical working scheme. This will verify if the total strain is a variable in the mechanical properties associated with this alloy.

2. Further research by TEM into the effects of strain hardening and grain size strengthening mechanism on the heavier rolled reduction scheme during the warm rolling process. This study will essentially allow optimization of the superplastic properties of this alloy.

# APPENDIX A

## MECHANICAL TEST DATA ON Al-10%Mg-0.1Zr ALLOY

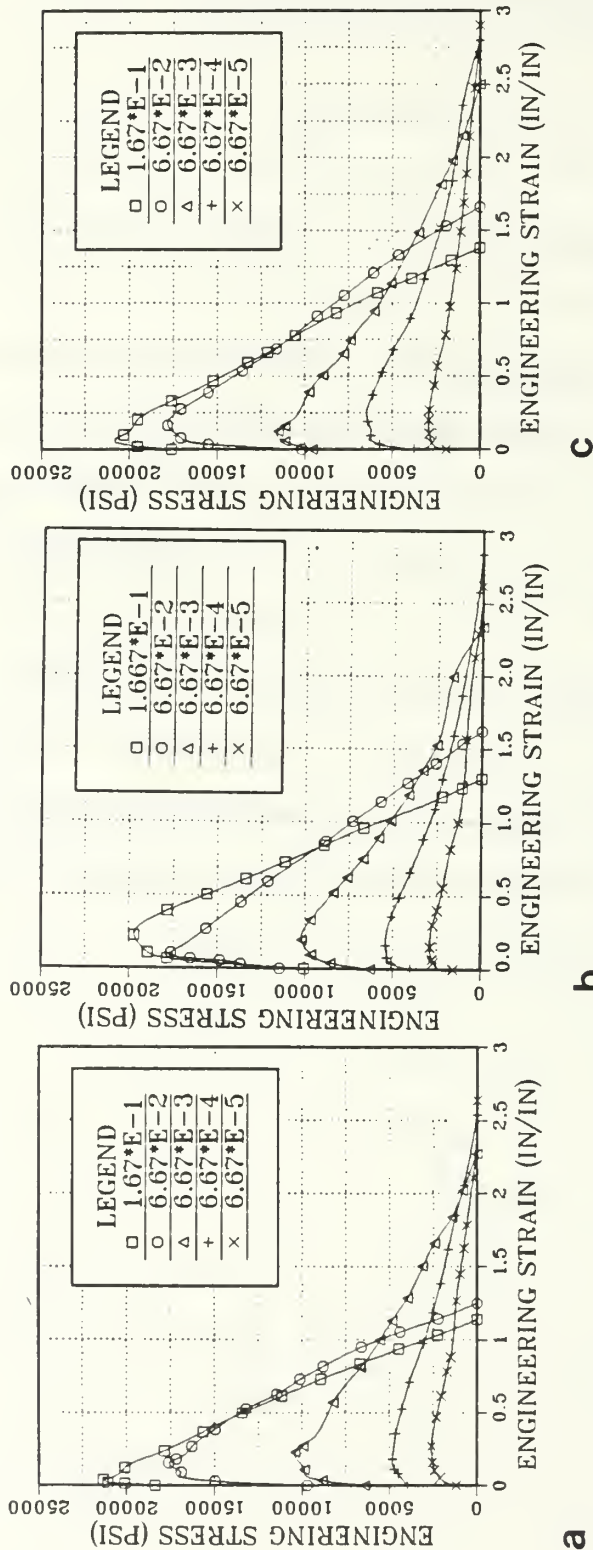


Figure A.1. Engineering stress versus engineering strain data for tension testing conducted at 300°C for the heavy reduction processing material warm rolled at 300°C to 85 percent reduction; (a) annealed 1 hr. at 200°C, (b) annealed 10 hrs. at 200°C, (c) annealed 1 hr. at 300°C.



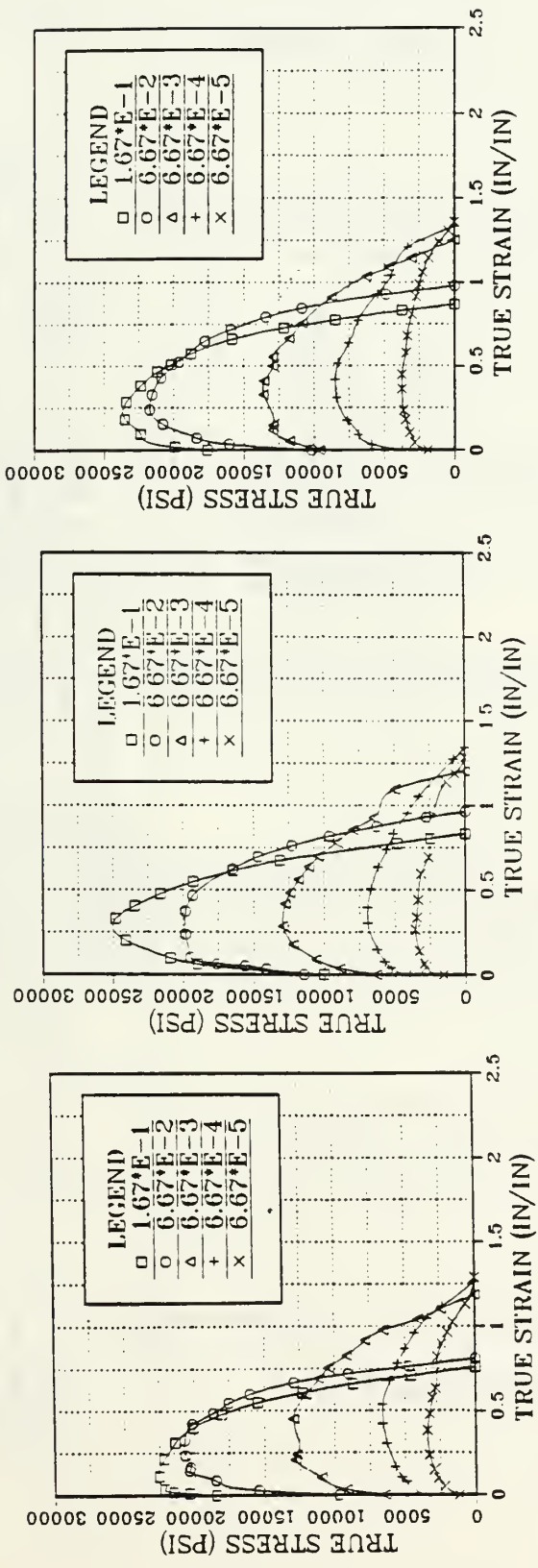


Figure A.2. True stress versus true strain data for tension testing conducted at 300 C for the heavy reduction processing material warm rolled at 300 C to 85 percent reduction; (a) annealed 1 hr. at 200°C, (b) annealed 10 hrs. at 200°C, (c) annealed 1 hr. at 300°C.

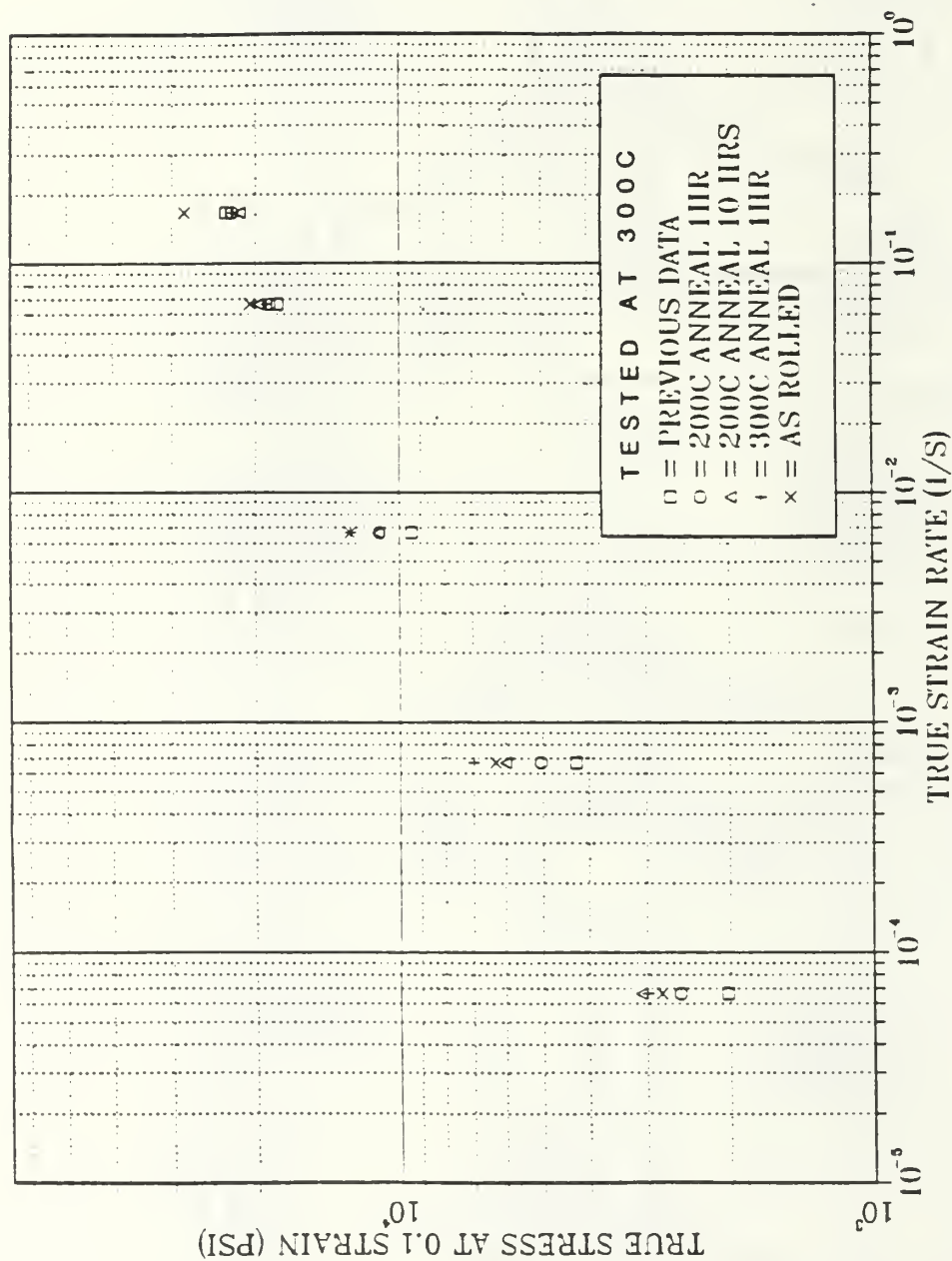


Figure A.3. True stress at 0.1 strain versus true strain data for tension test conducted at 300°C; specimens warm rolled at 300°C to 85 percent reduction using the heavy reduction processing of material. Comparison is made with previous data, the previous material was warm rolled at 300°C to 92 percent reduction using a light reduction scheme. The heavy reduction specimens were also annealed at various temperatures and times.

APPENDIX B  
COMPUTER PROGRAM

```
10 INPUT "WHAT FILENAME.<FT> DO YOU WISH TO USE ";ID$
20 INPUT "SAMPLE ID..",ID$
30 INPUT "SCALE FACTOR..",SCALE
40 INPUT "CROSSECTIONAL AREA CU. IN..",AO
50 INPUT "MAGNIFICATION RATIO..",MAG
60 OPEN "O",#1,D$
70 INPUT "ENTER THE LOAD,LBF..",F
80 INPUT "ENTER X MEASURE FROM CHART,IN..",DELX
90 S=F/AO
100 DELL=(DELX*SCALE)/MAG
110 E=DELL/1
120 SIGMA=S*(1+E)
130 EPSILON=LOG(1+E)
140 WRITE #1,F,DELX,S,E,SIGMA,EPSILON
150 INPUT "HIT RETURN TO CONT..N NEW SPECIMEN,OR Q..",ANS$
160 IF ANS$="" GOTO 70
170 IF ANS$="N" THEN CLOSE #1:CLS:GOTO 10
180 IF ANS$="Q" THEN CLOSE #1:GOTO 190
190 END
```

## LIST OF REFERENCES

1. Askland, D.E., The Science and Engineering of Materials, Brooks/Cole Engineering Division, 1984.
2. Johnson, R.B., The Influence of Alloy Composition and Thermomechanical Processing Procedure on Microstructural and Mechanical Properties of High-Magnesium Aluminum Alloys, M.S. Thesis, Naval Postgraduate, Monterey, California, June 1980.
3. Sherah, R.H., The Influence of Solution Time and Quench Rate on the Microstructure and Mechanical Properties of High-Magnesium Aluminum Magnesium Alloys, M.S. Thesis, Naval Postgraduate School, Monterey, California, December 1981.
4. McNelley, T.R. and Garg, A., "Development of Structure and Mechanical Properties in Al-10.2 Mg by Thermomechanical Processing", Scripta Metallurgical, Vol. 18, pp. 917-920, 1984.
5. Johnson, R.H., "Superplasticity", Metallurgical Reviews, Review 146; Vol 15, pp. 115-134, 1970.
6. Sherby, O.D. and Wadsworth, J., "Development and Characterization of Fine-Grain Superplastic Materials", Deformation, Processing, and Structure, pp. 354-384, 1982.
7. Klankowski, K.A., Retained Ambient Temperature Properties of Superplastically Deformed Al-10%Mg-0.1Zr, Al-10%Mg-0.5%Mn and Al-10%Mg-0.4%Cu Alloys, M.S. Thesis, Naval Postgraduate School, Monterey, California, December 1985.
8. Wert, J.A., "Thermomechanical Processing of Heat-Treatable Aluminum Alloys for Grain Size Control", Conference Proceedings of TMS-AIME, pp. 67-94, February 1985.
9. Dieter, G.E., Materials Science and Engineering Series, McGraw-Hill, 1976.
10. Wert, J.A., "Grain Refinement and Grain Size Control", Superplastic forming of structure alloys, Conference Proceedings of TMS-AIME, pp. 69-83, June 1982.
11. Gurland, J., "Application of the Hall-Pitch Relation to Particle Strengthening in Spheroidized Steels and Aluminum-Silicon Alloys", Conference Proceedings of Second ICMA, Vol 2., pp. 621-625, September 1970.



12. McNelley, T.R., Lee, E.W. and Mills, M.E., Superplasticity in a Thermomechanically Processed High-Mg, Al-Mg Alloy, in press, Metallurgical Transactions.
13. Lee, E.W., McNelley, T.R. and Stengel, A.F., The Influence of Thermomechanical Processing Variables on Superplasticity in a High-Mg, Al-Mg Alloy, in press, Metallurgical Transactions.
14. Stengall, M.J., "Cavitation in Superplasticity", Superplastic Forming of Structure Alloys, Conference Proceedings of TMS-AIME, pp. 321-336, June 1982.
15. Davis, G.J., Edington, C.P., Cutler, C.P., Padmanabhan, K.A., "Superplasticity", Journal of Materials Science; Vol. 5, pp. 1091-1102.
16. Ruano, O.A. and Sherby, O.D., "Low Stress Creep of Fine-Grain Materials at Intermediate Temperatures: Diffusional Creep on Grain Boundary Sliding?", Materials Science and Engineering, Vol. 56, pp. 167-175, 1982.
17. Alcamo, M.E., Effect of Strain and Strain Rate of Microstructure of a Superplastically Deformed Al-10%Mg-0.1%Zr Alloy, Mechanical Engineer Thesis, Naval Postgraduate School, Monterey, California, June 1985.
18. Berthold, D.B., "Effect of Temperature and Strain Rate on the Microstructure of a Deformed, Superplastic Al-10%Mg-0.1%Zr Alloy", M.S. Thesis, Naval Postgraduate School, Monterey, California, June 1985.
19. Hartman, T.S., Mechanical Characteristics of a Superplastic Aluminum-10%Mg-0.1%Zr Alloy, M.S. Thesis, Naval Postgraduate School, Monterey, California, June 1985.
20. Alcoa Technical Center, Ltr., August 1984.
21. Becker, J.J., Superplasticity in Thermomechanically Processed High-Magnesium Aluminum Magnesium Alloys, M.S. Thesis, Naval Postgraduate School, Monterey, California, March 1984.
22. Mills, M.E., Superplasticity in Thermomechanically Processed Aluminum-10%Mg-0.52Mn Alloy, M.S. Thesis, Naval Postgraduate School, Monterey, California, September 1984.
23. Metals Handbook, 9th ed., Vol. 9, pp. 351-360, American Society for Metals, 1985.

24. Pashly, D.W., "The Development and Use of Superplastic Aluminum Alloy", Metal, Vol. 34, pp. 307-311, 1980.
25. McNelley, T.R., Lee W.E., Garg A., Superplasticity in Thermomechanical Processed High-Mg, Al-Mg-X Alloys.  
Submitted to International Conference on Aluminum Alloys.

# INITIAL DISTRIBUTION LIST

	No. Copies
1. Defense Technical Information Center Cameron Station Alexandria, Virginia 22304-6145	2
2. Library, Code 0142 Naval Postgraduate School Monterey, California 93943-5000	2
3. Department Chairman, Code 69Mx Department of Mechanical Engineering Naval Postgraduate School Monterey, California 93943-5000	1
4. Professor T.R. McNelley, Code 69Mc Department of Mechanical Engineering Naval Postgraduate School Monterey, California 93943-5000	5
5. Dr. Steve J. Hales, Code 69He Department of Mechanical Engineering Naval Postgraduate School Monterey, California 93943-5000	1
6. Jeff Waldman Naval Air Development Center Materials Science Department Warminster, Pennsylvania 18974	1
7. Dr. Eu Whee Lee Naval Air Development Center Materials Science Department Warminster, Pennsylvania 18974	1
8. LT William H. Grider, USN Supervisor of Shipbuilding, Conversion and Repair, USN Pascagoula, Mississippi 39567	4















DUDLEY KNOX LIBRARY  
NAVAL POSTGRADUATE SCHOOL  
MONTEREY, CALIFORNIA 93943-5002

Thesis  
G7671  
c.1

Grider

The effect of thermo-  
mechanical processing  
variables on ductility  
of a high-Mg, Al-Mg-Zr  
alloy.

218744

Thesis

G7671 Grider

c.1

The effect of thermo-  
mechanical processing  
variables on ductility  
of a high-Mg, Al-Mg-Zr  
alloy.

218744

thesG7671

The effect of thermomechanical processin



3 2768 000 67035 0

DUDLEY KNOX LIBRARY